Martin Marietta Laboratories

MML TR 86-76c

SURFACE AND INTERFACE CHARACTERIZATION FOR HIGH-TEMPERATURE ADHESIVE SYSTEMS

Annual Report

Period:
September 1, 1985, to August 31, 1986

Prepared by:

D.K. Shaffer, H.M. Clearfield, J.S. Ahearn

Submitted to:

Department of the Navy
Office of Naval Research
Arlington, Virginia 22217

Under Contract No. N00014-85-C-0804

Submitted by:

MARTIN MARIETTA CORPORATION
Martin Marietta Laboratories
1450 South Rolling Road
Baltimore, Maryland 21227

September 1986

REPORT DOCUMENTATION PAGE

READ INSTRUCTIONS BEFORE COMPLETING FORM

1. REPORT NUMBER: MML TR 86-76(c)	2. GOVT ACCESSION NO. / 3. RECIPIENT'S CATALOG NUMBER
4. TITLE (and Subtitle): Surface and Interface Characterization for High-Temperature Adhesive Systems	5. TYPE OF REPORT & PERIOD COVERED: Annual Report, Sept. 1, 1985 - Aug. 31, 1986
	6. PERFORMING ORG. REPORT NUMBER
7. AUTHOR(s): D.K. Shaffer, H.M. Clearfield, J.S. Ahearn	8. CONTRACT OR GRANT NUMBER(s): N00014-85-C-0804
9. PERFORMING ORGANIZATION NAME AND ADDRESS: Martin Marietta Laboratories, 1450 S. Rolling Road, Baltimore, Maryland 21227	10. PROGRAM ELEMENT, PROJECT, TASK AREA & WORK UNIT NUMBERS
11. CONTROLLING OFFICE NAME AND ADDRESS: Department of the Navy, Office of Naval Research, Arlington, VA 22217	12. REPORT DATE: September 1986 / 13. NUMBER OF PAGES: 49 (incl 22 text)
14. MONITORING AGENCY NAME & ADDRESS (if different from Controlling Office)	15. SECURITY CLASS. (of this report): Unclassified / 15a. DECLASSIFICATION/DOWNGRADING SCHEDULE

16. DISTRIBUTION STATEMENT (of this Report)

Unlimited - Approved for Public Release

17. DISTRIBUTION STATEMENT (of the abstract entered in Block 20, if different from Report)

18. SUPPLEMENTARY NOTES

19. KEY WORDS (Continue on reverse side if necessary and identify by block number)

Adhesive Bonding
Titanium Oxide
High-Temperature Adhesives

20. ABSTRACT (Continue on reverse side if necessary and identify by block number)

The structural and bonding properties of Ti-6Al-4V adherends, prepared by chromic acid anodization (CAA), were studied as a function of exposure in high-temperature environments such as vacuum, air, boiling and pressurized water, and steam. Subsequent to the environmental exposure, bonds were produced and the adhesive tensile strengths measured. Long-term exposure to high temperature, dry environments did not cause structural changes to the adherend oxide but did result in poor bond strength. The failure mode in these cases was within the oxide, which was apparently weakened by the exposure. The water- and steam-exposed oxides

underwent a transition from amorphous to crystalline TiO_2 (with an accompanying change in oxide morphology); however, bond strength was maintained for moderate exposures at T 300°C. For exposure at T=300°C, the bond strength was degraded severely. The latter result can be explained by a lack of porosity in the transformed oxide. SEM and XPS measurements were made on debonded surfaces to determine the loci of failure. The results from investigations of two alternative adherend surface preparations, i.e., anodization in sodium hydroxide (for Ti-6Al-4V) and the application of an Al alkoxide primer (for Al 2024), are also reported.

MML TR 86-76c

SURFACE AND INTERFACE CHARACTERIZATION FOR HIGH-TEMPERATURE ADHESIVE SYSTEMS

Annual Report

September 1, 1985, to August 31, 1986

Submitted to:

Department of the Navy
Office of Naval Research
Arlington, Virginia 22217

Under Contract No. N00014-85-C-0804

Accesion For	
NTIS CRA&I	☑
DTIC TAB	☐
Unannounced	☐
Justification	
By	
Distribution /	
Availability Codes	
Dist	Avail a d / or Special
A-1	

Submitted by:

D.K. Shaffer, H.M. Clearfield, J.S. Ahearn
MARTIN MARIETTA CORPORATION
Martin Marietta Laboratories
1450 South Rolling Road
Baltimore, Maryland 21227

September 1986

PREFACE

A major portion of the body of this report is derived from the preprint submitted for the International Adhesion Society meeting, February 22-27, 1987, in Williamsburg, Virginia.

TABLE OF CONTENTS

ABSTRACT

The structural and bonding properties of Ti-6Al-4V adherends, prepared by chromic acid anodization (CAA), were studied as a function of exposure in high-temperature environments such as vacuum, air, boiling and pressurized water, and steam. Subsequent to the environmental exposure, bonds were produced and the adhesive tensile strengths measured. Long-term exposure to high temperature, dry environments did not cause structural changes to the adherend oxide but did result in poor bond strength. The failure mode in these cases was within the oxide, which was apparently weakened by the exposure. The water- and steam-exposed oxides underwent a transition from amorphous to crystalline TiO_2 (with an accompanying change in oxide morphology); however, bond strength was maintained for moderate exposures at $T < 300°C$. For exposure at $T=300°C$, the bond strength was degraded severely. The latter result can be explained by a lack of porosity in the transformed oxide. SEM and XPS measurements were made on debonded surfaces to determine the loci of failure. The results from investigations of two alternative adherend surface preparations, i.e., anodization in sodium hydroxide (for Ti-6Al-4V) and the application of an Al alkoxide primer (for Al 2024), are also reported.

I. INTRODUCTION

Adhesively bonded materials that are stable at high temperatures are becoming increasingly important for the performance of advanced military and aerospace systems. The proposed operating temperature range, from 100-400°C, presents special problems for all components of the bonded system, i.e., adherend, primer, and adhesive must all be stable in severe environments. Several classes of metal adherends are used (or have been proposed) for such systems, including titanium alloys, nickel-based superalloys, and high-temperature steels. One, Ti-6Al-4V, is a particularly good baseline material for the adherend because its mechanical properties are retained at high temperatures.

In previous studies of both Ti [1] and Al [2,3] adhesive bonding systems, it was shown that initial bond strength was enhanced by physical interlocking between the adherend oxide and the adhesive; porous oxides maximized this interlocking and hence provided the best overall bond strength. Additionally, in Al adherends, humidity-induced changes in the oxide led to bond degradation. The primary cause of failure in that case was the transformation of the original oxide to a hydroxide that is loosely bound to the Al substrate [2]. Certain organic inhibitors were later used to slow down such a transformation, thereby increasing bond durability [3].

The oxide of Ti, typically formed by anodization in a chromic acid solution (CAA), is much more stable than that of Al and hence the bonds exhibit markedly better durability. However, the unbonded Ti oxide was found to undergo a transition from amorphous TiO_2 to crystalline TiO_2 (anatase) when immersed in water at 85°C for as little as 20 hours [4]. The transformation was accompanied by a change in morphology -- from a porous, honeycomb structure to a more needle-like structure. Although some porosity was retained after this transformation, it was later shown that exposure to humid environments for longer times or at higher temperatures results eventually in a rather smooth, nodular-like oxide that lacks porosity [5]. The effects of various environmental exposures on the oxide thickness have also been reported [6].

The observation that a CAA oxide that was transformed at lower temperatures retained porosity suggests that such an oxide might couple mechanically to an adhesive. It would be desirable to use such a transformed oxide in a bond line, if the oxide-base metal interfacial strength were maintained, because the crystalline Ti oxide phases are more stable thermodynamically than the amorphous phase [7]. Although anatase is not the most stable form of TiO_2 [7], none of the other crystalline TiO_2 phases has been observed in earlier Ti adherend studies [4,5]. Thus, by bonding to a crystalline adherend oxide, i.e., anatase, large-scale morphology changes that normally occur during accelerated testing could presumably be avoided, thereby increasing bond durability.

In this study, we have investigated the strength of bonds formed on Ti-6Al-4V adherends after they were subjected to high-temperature environments such as vacuum, air, boiling water, pressurized water and steam. The CAA oxide was chosen as the baseline adherend because it provides excellent bond durability for Ti adhesive bonds [1]. Coupons were anodized, exposed, bonded to an Al stud (see below), and tested with an instrument that applies a tensile force normal to the adherend surface. The test was designed to determine the adhesion of the (transformed) oxide to the underlying substrate. Adherends were characterized before and after tensile testing by high-resolution scanning electron microscopy (SEM) and x-ray photoelectron spectroscopy (XPS). These measurements allowed the identification of the loci of failure in the adhesion tensile tests. The failure mechanisms were then correlated with the respective oxide morphologies.

The evaluation of one alternative surface preparation, based on anodization of the Ti-6Al-4V in sodium hydroxide [8], was conducted, in order to investigate the adhesive bonding properties of adherend surfaces prepared in a nonacidic medium. These specimens were subsequently characterized before and after environmental exposures and tensile testing for comparison with the CAA surfaces. In a recent study, the ability of an Al alkoxide coating to improve

the bond durability of Al adherends by chemical coupling [9] was investigated. The results of wedge tests, performed to evaluate the alkoxide with different surface preparations of varying morphology on Al 2024 adherends, are reported.

II. EXPERIMENTAL

A. SAMPLE PREPARATION

Coupons of Ti-6Al-4V were anodized in a solution containing 5% chromic acid (CAA). Details of the procedure are given elsewhere [5,10]. Transmission electron micrographs show that the resultant oxide is ~ 1200 Å thick and amorphous [5]. Specimens anodized in sodium hydroxide solutions of varying concentration, temperature, and voltage conditions were prepared according to the method of Kennedy et al. [8].

Coupons subjected to heat alone were placed in a vacuum furnace for periods of 72 and 160 hr at 400°C, and at a pressure of 2×10^{-6} torr. Although there was no residual gas analyzer on the furnace, we estimate the partial pressure of oxygen to be less than 4×10^{-7} torr [11]. Any residual water vapor was pumped away during warmup. Additionally, some coupons were exposed to air in an ordinary laboratory furnace at 330°C. Exposure times varied from 160-1200 hr. The relative humidity in the furnace was not determined.

The boiling water exposures were conducted by immersion of the coupons in water maintained at 95-100°C. For higher temperature water exposures, a high-pressure autoclave was used. In this case, a sufficient volume of water was used at each temperature to maintain an equilibrium between liquid and vapor at the saturation vapor pressure. Some coupons were immersed in the liquid; others were exposed only to the vapor. Exposures ranged from 3-120 hr at temperatures of 150, 200, 250 and 300°C.

B. ADHESION TESTING

A pneumatic adhesion tensile testing instrument (SEMicro, Rockville, MD) was used for the adhesion tests. A schematic drawing of the testing geometry is shown in Fig. 1. A 1.25-cm-diameter Al stud (that had been etched

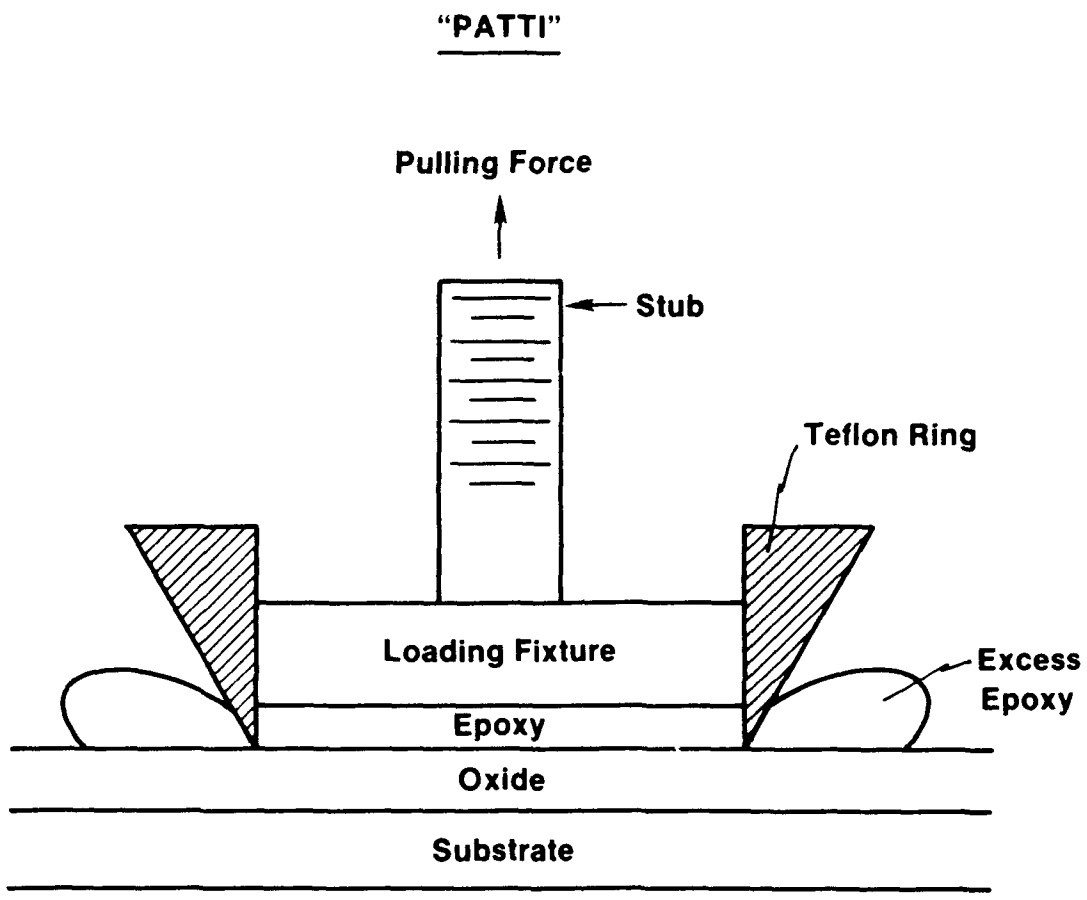

Figure 1. Schematic diagram of adhesion tensile testing geometry.

previously in FPL solution) was bonded to the pre-exposed adherend with an epoxy resin (3M 1838). The bonding area was defined with a Teflon ring. The adhesive was cured under pressure for 72 hr at room temperature. Prior to testing, the Teflon ring was replaced by a stainless steel ring and the bonded system was mounted in a jig that prevents the adherend from flexing. The stud was screwed into a pneumatic piston which applies the tensile force normal to the adherend surface. The force required to remove the stud thus provides a relative indication of the bond strength of the oxide.

C. ANALYSIS

A JEOL JEM 100-CX STEM, used in the SEM mode, provided the resolution needed to examine the morphology of the CAA and SHA oxides and the bond-failure surfaces. Samples were cut to 1 cm x 2 mm and coated with ~ 50 Å of Pt to eliminate charge buildup on the oxide. The stereo micrographs shown in this study were obtained at ± 7 deg tilt.

XPS was used to determine the surface composition of the oxides and the debonded surfaces. The spectrometer, an SSL SSX-100, was equipped with a differentially pumped ion sputter gun. For compositional analysis, the analyzed area was 600 μm in diameter, which was large enough to represent the average over the entire coupon surface. For depth profiles, a 300-μm-diameter area at the center of a 3 mm X 3 mm crater was used.

III. RESULTS AND DISCUSSION

A. MORPHOLOGY OF EXPOSED ADHEREND

The process for producing a consistent CAA oxide has been reported [5]. A stereo micrograph of a typical, as-anodized CAA oxide is shown in Fig. 2. It is characterized by a multilevel, porous structure with cell dimensions on the order of 400 Å. At lower magnifications (Fig. 2a), it is evident that the porous structure covers the entire surface. The multilevel morphology is presumably due to differential etching of the two-phase alloy.

Samples that were exposed to vacuum at 400°C for as long as 160 hr (Fig. 3) showed no change in morphology when examined by SEM, i.e., the porous, honeycomb morphology was retained. However, for a sample exposed to air at 320°C for 1200 hr, Fig. 4, although the honeycomb structure is still evident, the cell walls have thickened slightly. Additionally, some peeling of the oxide seems to have occurred at the grain boundaries.

CAA oxides immersed in boiling water developed crystallites, consistent with earlier results [1,4]. After as little as 3-hr immersion, the honeycomb cell walls begin to thicken (Fig. 5). By 24 hr (Fig. 6), crystallites can be observed and the cells have nearly closed up and by 72 hr (Fig. 7.), the adherend surface is covered with crystallites and the honeycomb structure has disappeared. Some fusion of the crystallites has also occurred.

As already mentioned, some CAA oxides exposed to water in the autoclave were immersed in the liquid, while others that hung above the liquid were exposed only to the vapor. The evolution of the oxide is different for the two exposures, as can be seen in the sequence of Figs. 8-10. Those immersed in the liquid at 300°C were completely covered by needle-like crystallites after as little as 3 hr (Fig. 8). By 24 hr (Fig. 9), the crystallites began to fuse and the surface appears somewhat flatter. Finally, after 120 hr (Fig. 10),

5% CAA As-Anodized

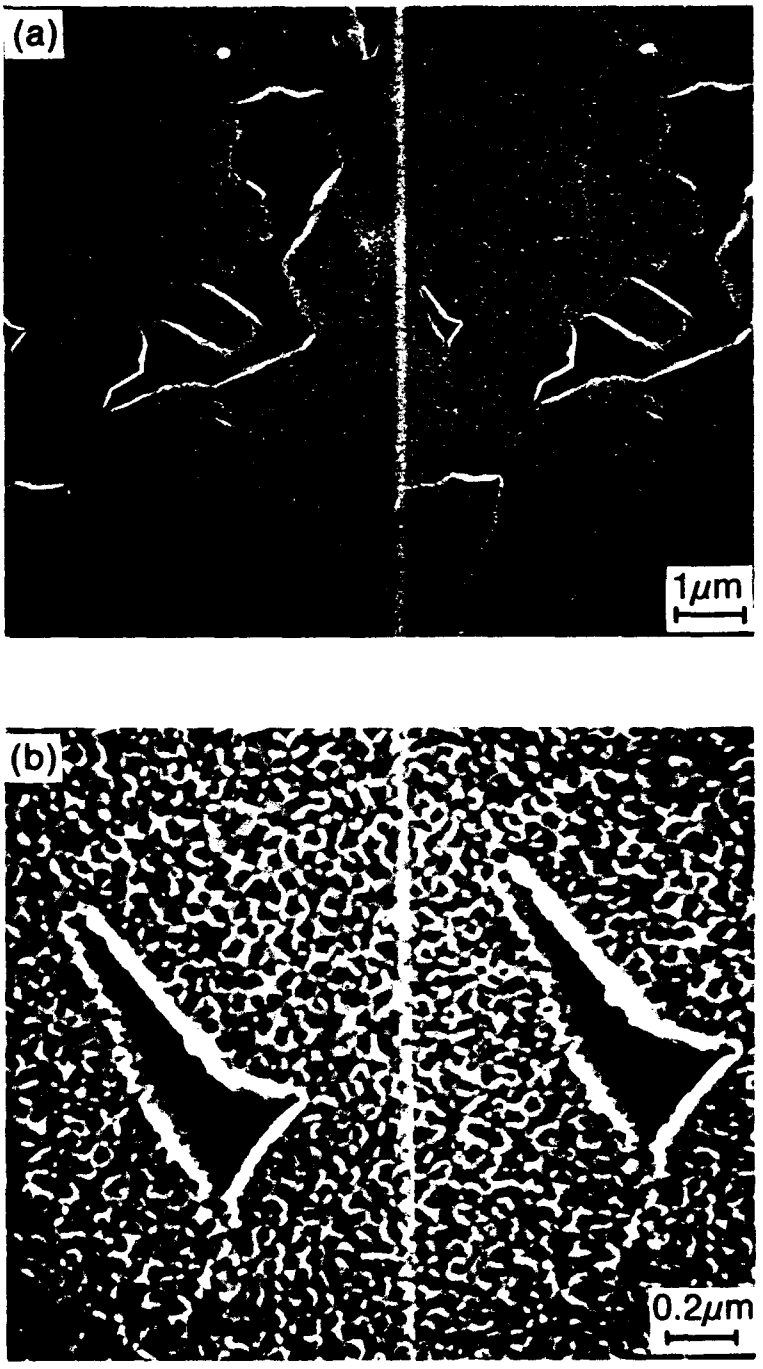

Figure 2. Scanning electron micrographs at (a) low and (b) high magnification, showing the CAA oxide surface resulting from the anodization of Ti-6Al-4V adherend in a solution containing 5% chromic acid.

Vacuum Exposure 400°C 165 hr

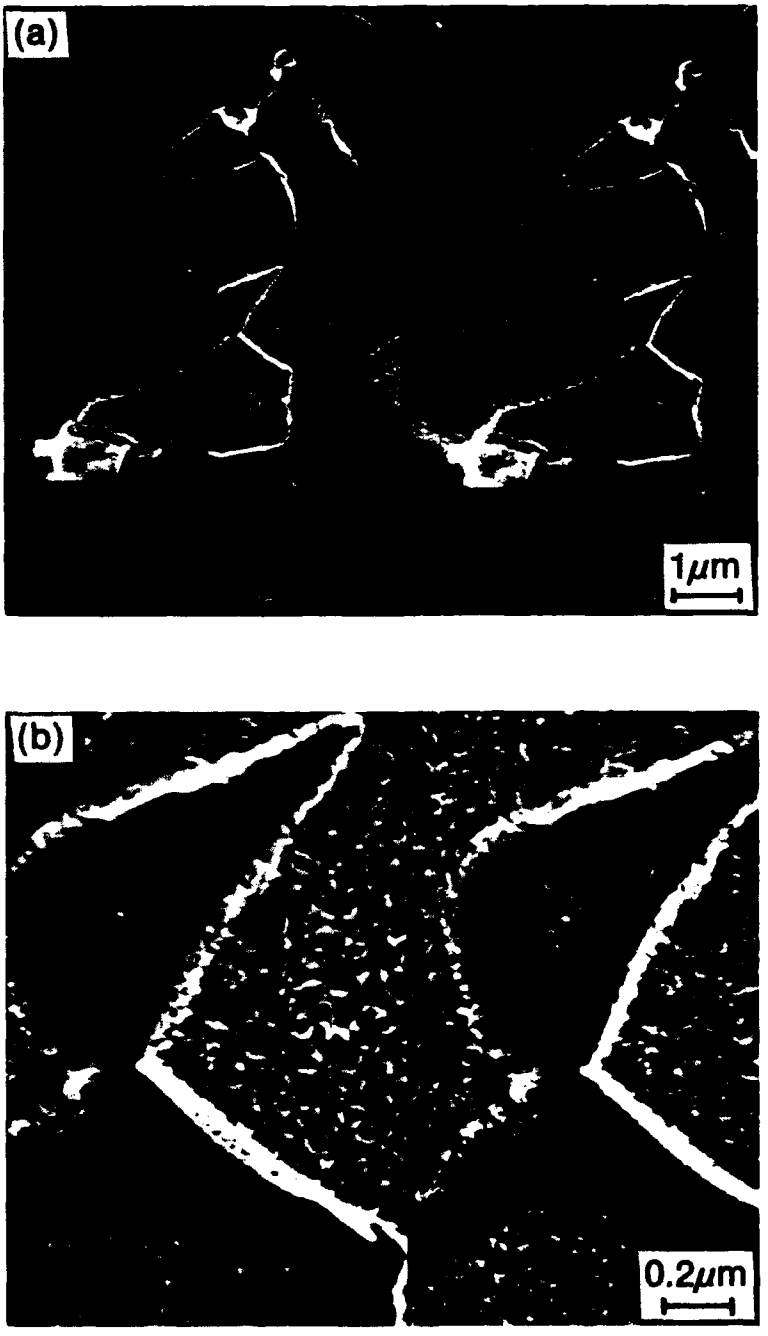

Figure 3. CAA oxide at (a) low and (b) high magnification, after heating in vacuum maintained at 400°C for 165 hours.

Air Exposure 320°C 1200 hr

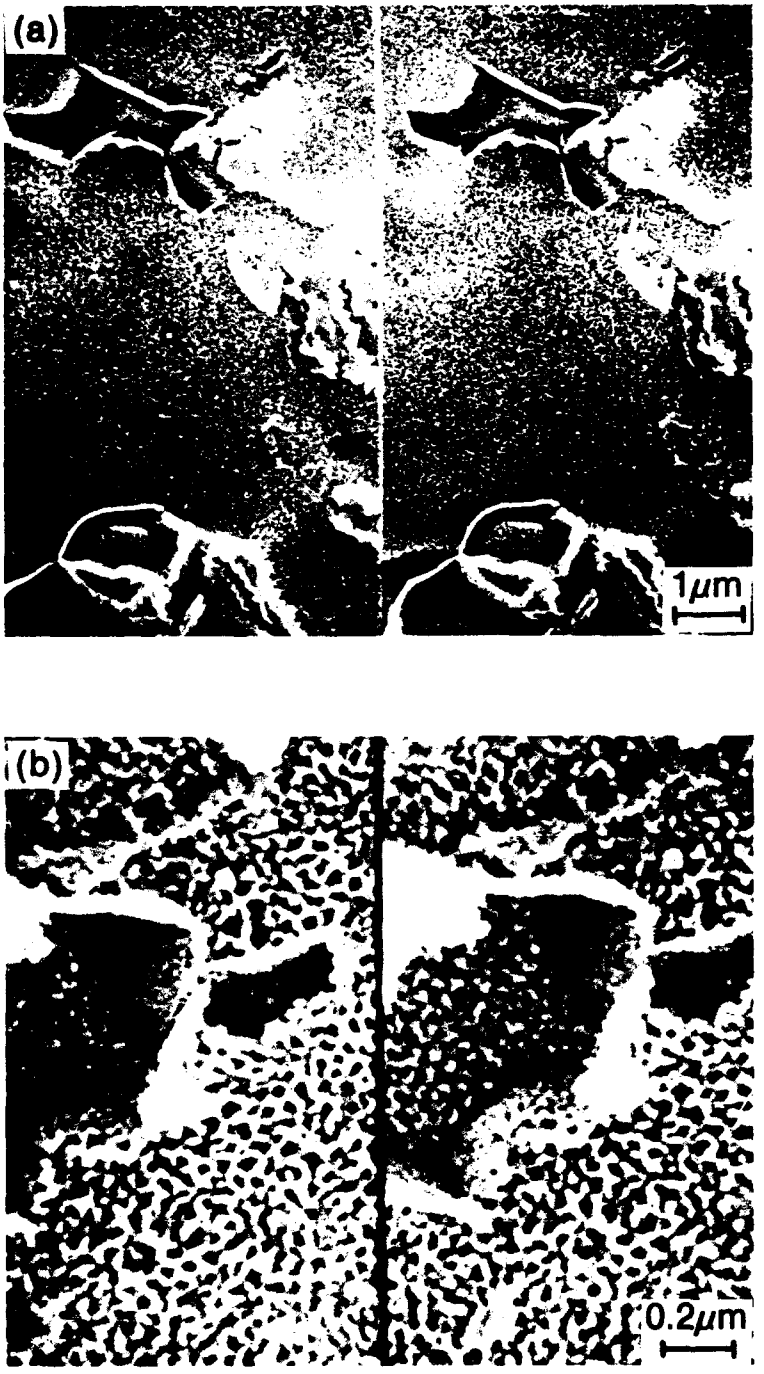

Figure 4. CAA oxide at (a) low and (b) high magnification, after heating in air maintained at 320°C for 1200 hours.

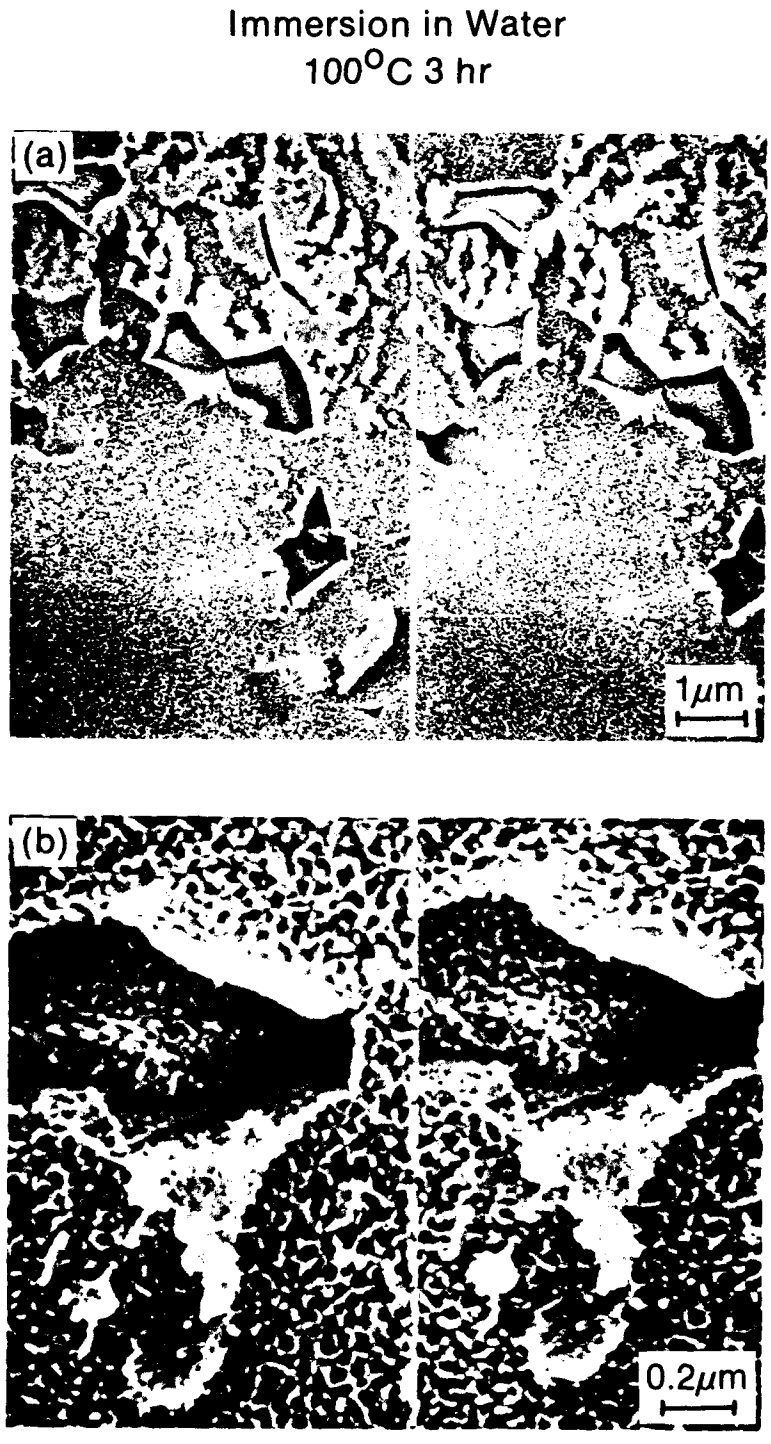

Figure 5. CAA oxide at (a) low and (b) high magnification, after immersion in water maintained at 100°C for 3 hours.

Immersion in Water
100°C 24 hr

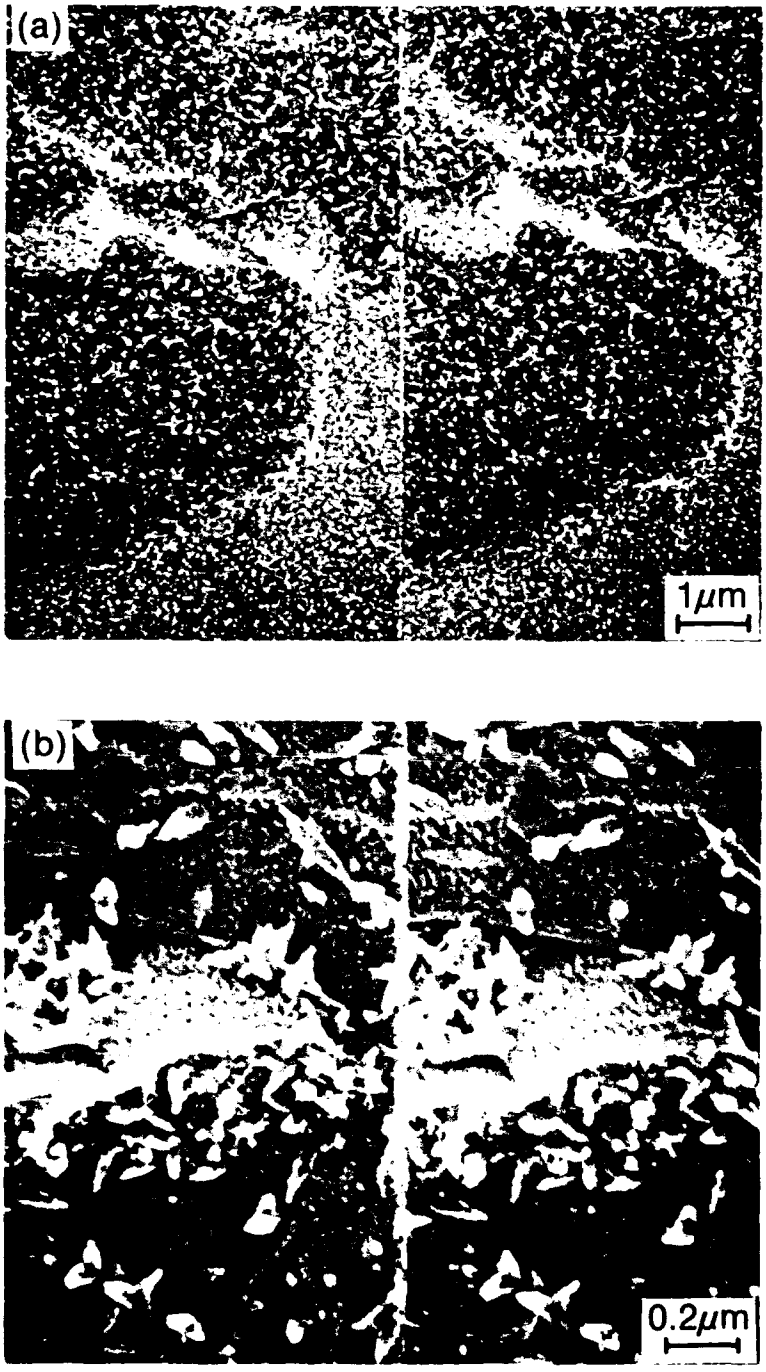

Figure 6. CAA oxide at (a) low and (b) high magnification, after immersion in water maintained at 100°C for 24 hours.

Immersion in Water
100°C 72 hr

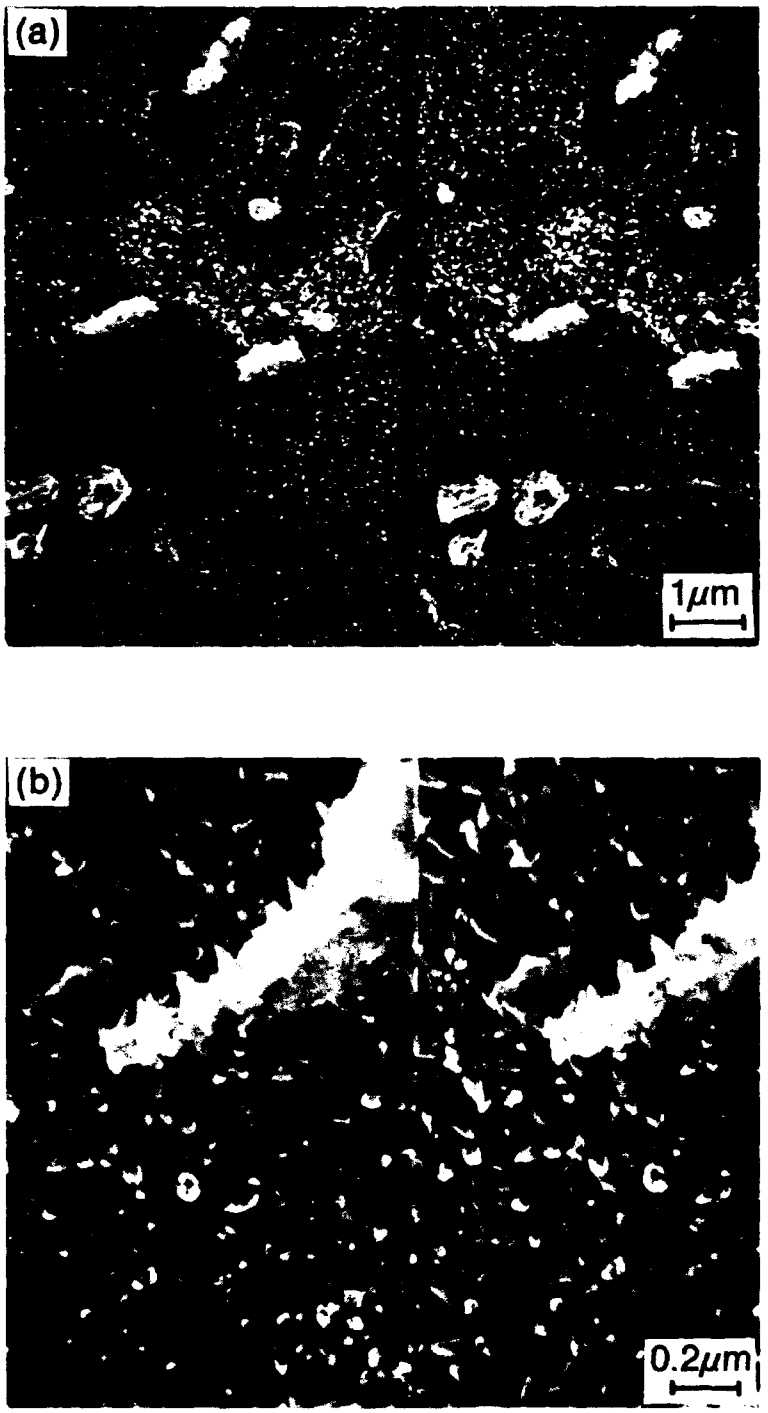

Figure 7. CAA oxide at (a) low and (b) high magnification, after immersion in water maintained at 100°C for 72 hours.

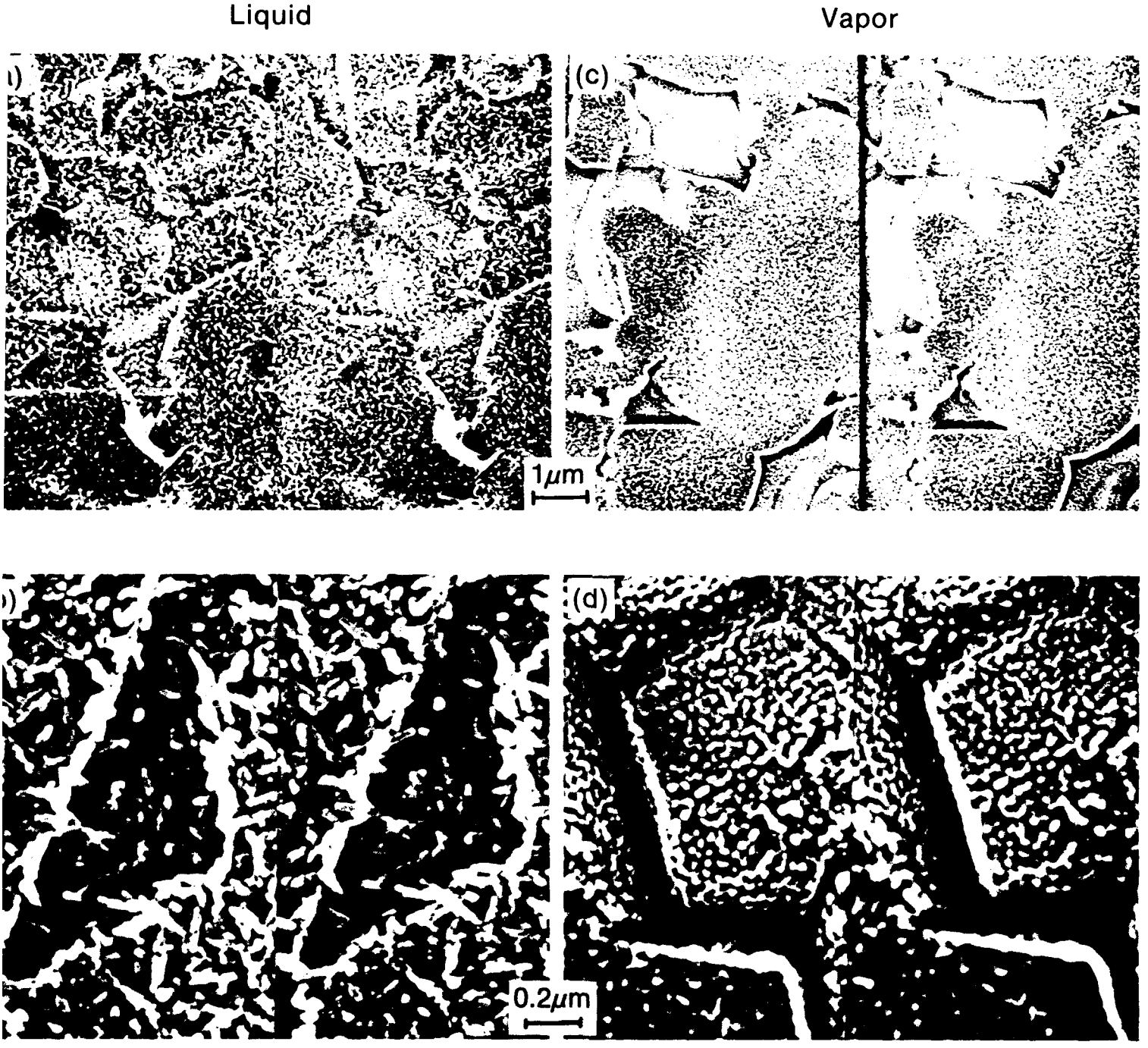

Figure 8. CAA oxide after exposure to water in the (a and b) liquid and (c and d) vapor phases, in an autoclave maintained at 300°C for 3 hours.

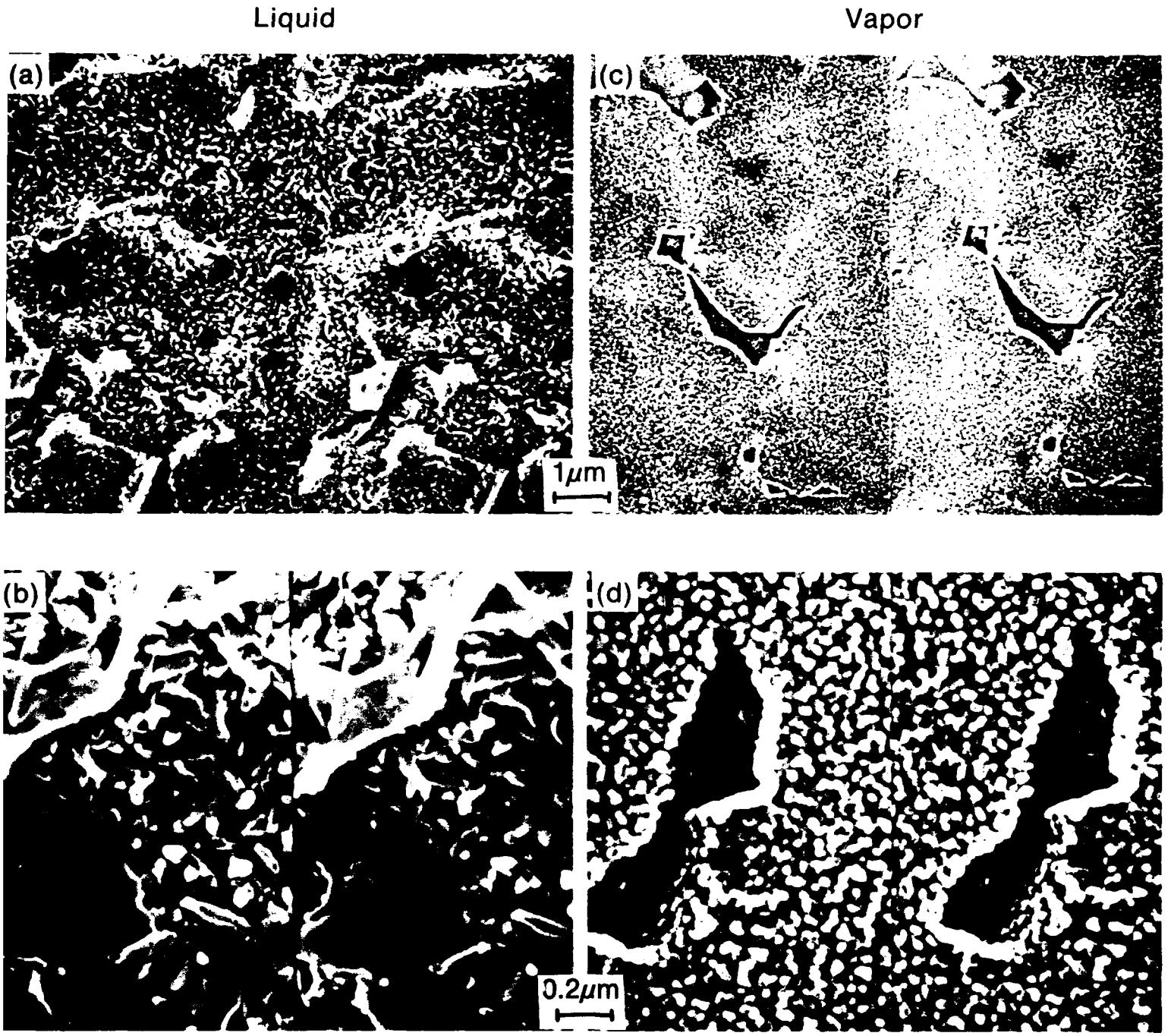

Figure 9. CAA oxide after exposure to water in the (a and b) liquid and (c and d) vapor phases, in an autoclave maintained at 300°C for 24 hours.

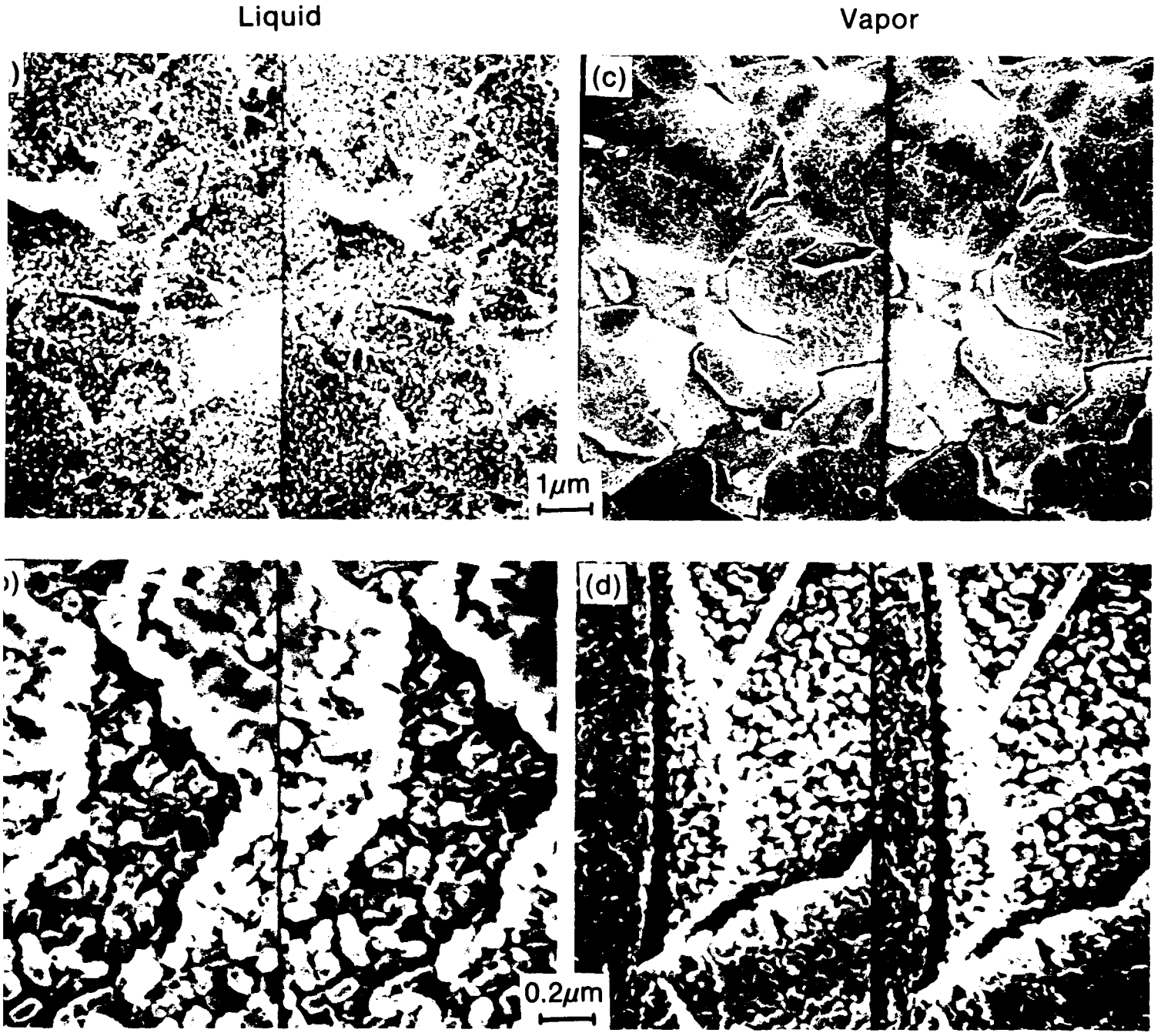

Figure 10. CAA oxide after exposure to water in the (a and b) liquid and (c and d) vapor phases, in an autoclave maintained at 300°C for 120 hours.

the crystallites had become nodular in shape, leaving an oxide that was relatively smooth (compared to the as-anodized oxide). For vapor-exposed oxides, no needle-like crystallites were observed. Rather, the honeycomb structure evolved into a more nodular-like oxide (Fig. 8). Selected area diffraction (SAD) patterns generated in the TEM show these nodules to be anatase TiO_2. With continued exposure, the nodules began to fuse (Fig. 9) until, by 120 hr, the oxide surface was again relatively smooth, i.e., not porous (Fig. 10). The diameter of the vapor-exposed nodules was approximately one-half that of the corresponding liquid-exposed nodules.

B. ADHESION TENSILE TESTS

The tensile test used in this study measured the relative adhesive strength of the oxide-base metal interface. The results are presented in Table I. The greatest bond strength was obtained with the as-anodized CAA oxide. Visual examination of the debonded surfaces showed both to have the same appearance -- rough and of the same color as the adhesive -- suggesting that the failure mode was cohesive. To confirm this, we examined the surfaces by SEM and XPS. The scanning electron micrographs showed an adhesive-like morphology on both sides with large (20-μm diameter; Fig. 11) filler particles consisting primarily of Al and Si. The XPS spectra obtained from the metal and the adhesive sides of the failure are nearly identical, as shown in Fig. 12. The C and O concentrations are indicative of adhesive material, and the Al and Si from the filler particles are evident. We conclude that 1340 psi (Table I) represents the cohesive strength of the adhesive under the test conditions.

Most of the high-temperature vacuum- and air-exposed specimens failed prior to testing as the Teflon ring was being removed. Those that were tested failed at pressures less than 100 psi. The debonded surfaces appeared metallic on both the stud and the metal sides, indicating failure entirely within the oxide layer or at the oxide-metal interface. The precise location was determined by SEM and XPS depth profiles. As seen in Fig. 13 (the stud side),

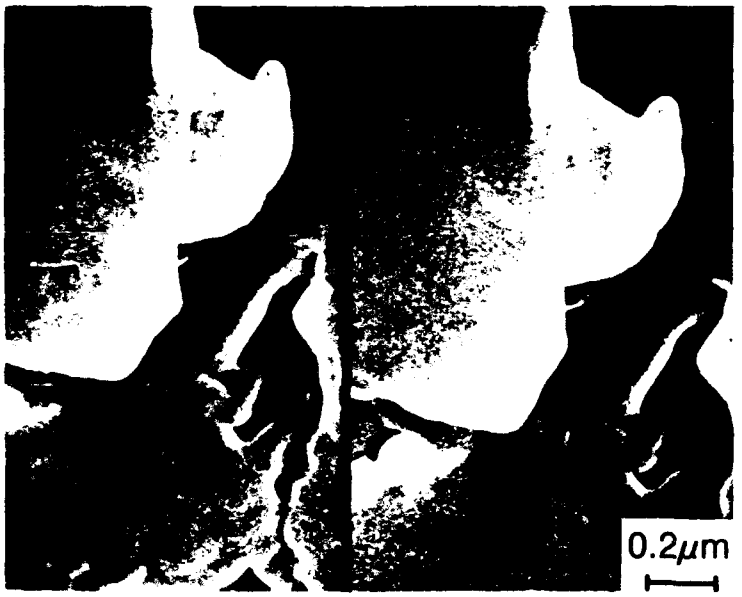

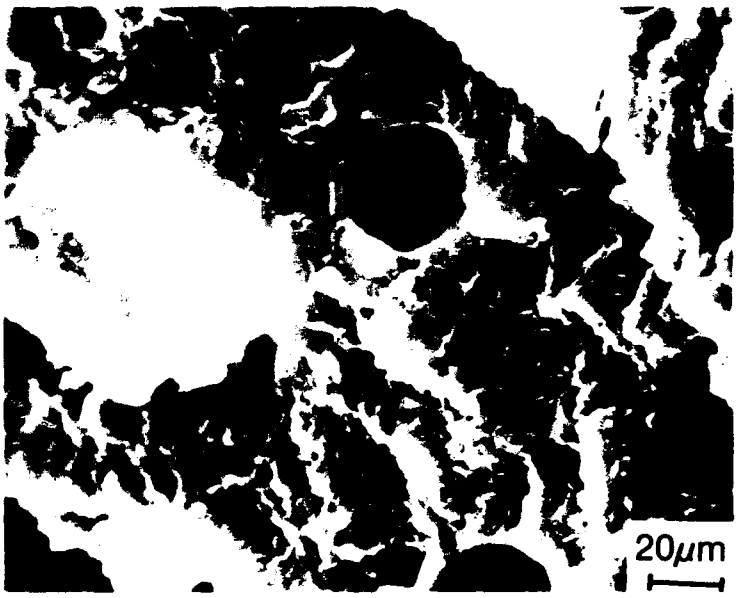

Figure 11. SEM micrographs showing adhesion pull surfaces from debonded CAA (as-anodized) system. Morphology indicates adhesive material found on both (metal and stub) sides of debonded surfaces.

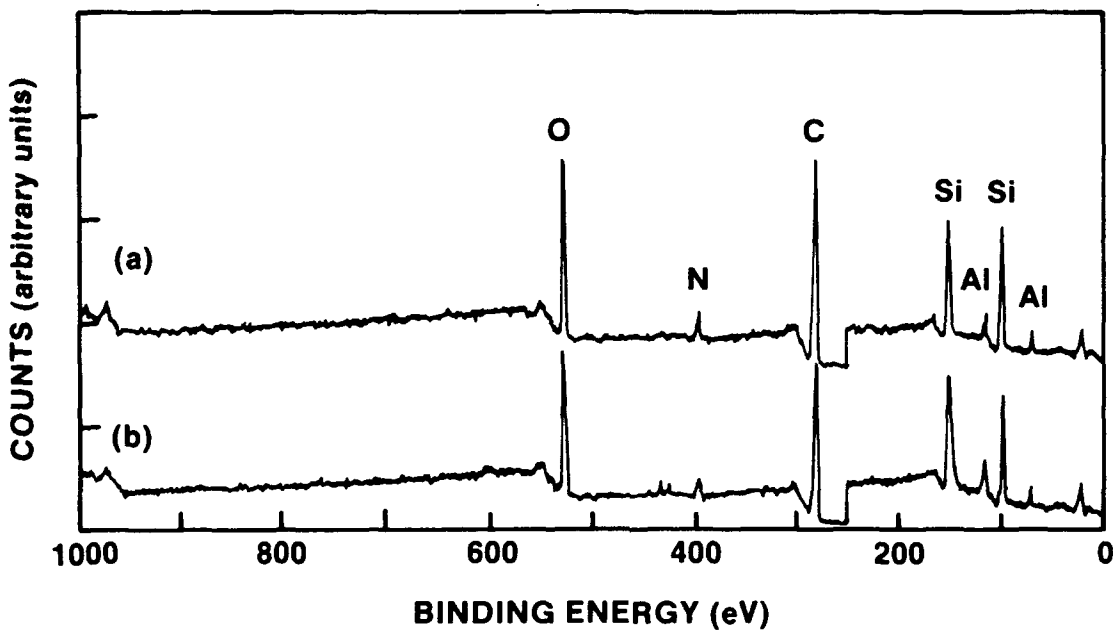

Figure 12. X-ray photoelectron spectra of a) metal and b) stud sides of an as-anodized Ti-6Al-4V adherend after tensile testing. The spectra are typical of adhesive.

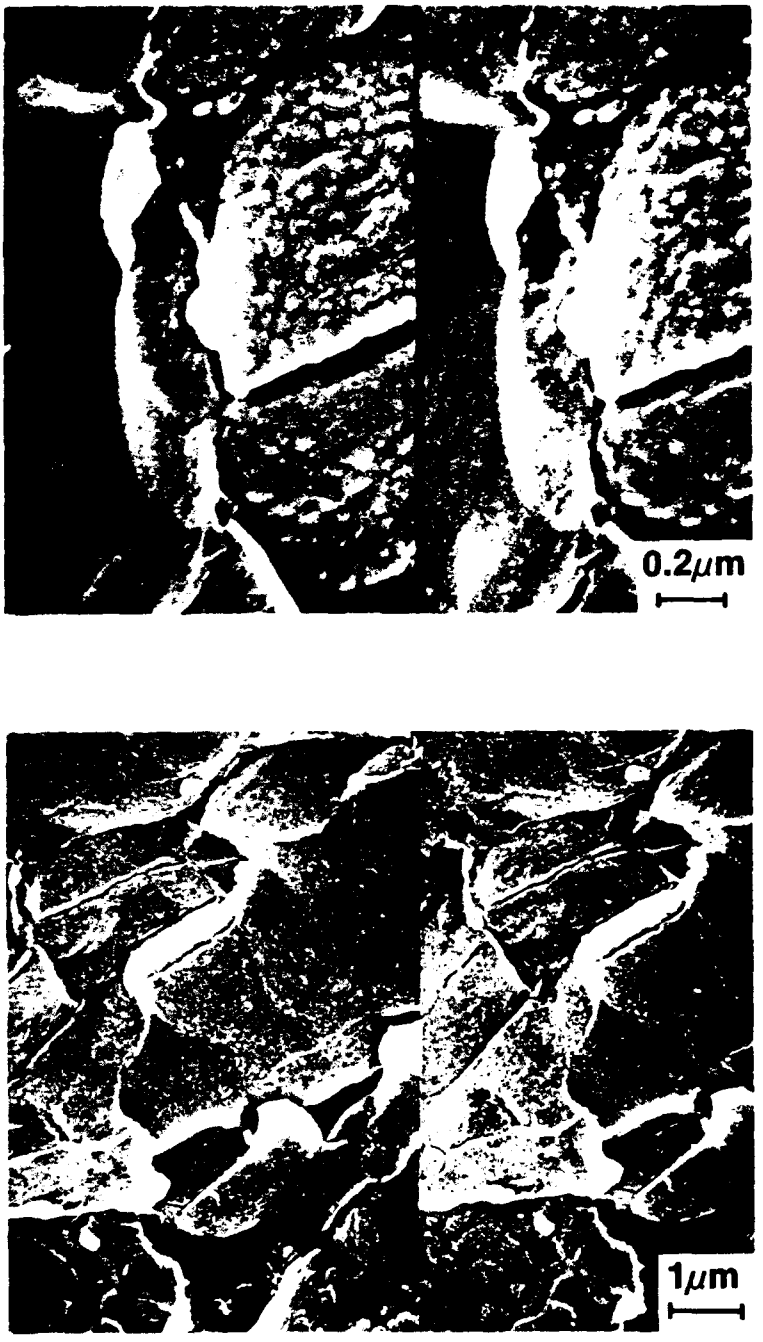

Figure 13. SEM micrographs showing adhesion pull surfaces from stub side of CAA adherend system after exposure in air at 330°C for 1200 hr. Failure occurred within the oxide layer, which is contained under the back side of barrier layer, as shown.

Table I. Adhesion tensile test results.

Ti-6Al-4V (CAA 5%)

EXPOSURE	PULL STRENGTH (psi)
As-anodized	1340 ± 70 (cohesive)*
Vacuum (T > 350°C)	0-100 (oxide)
Air 330°C, 165 hr	500 (mixed)
Air 330°C, 1200 hr	0-100 (oxide)
Water, steam (T < 300°C)	1200 (mixed)
Water, steam (T > 300°C)	0-100 (adhesive)

---

* Failure mode is indicated in parentheses.

the original CAA oxide cell walls are evident and have lifted away from the base metal. The micrograph from the metal side shows a complementary image. XPS survey spectra of both surfaces were identical; however, depth profiles (Fig. 14) show different oxide layer thicknesses. On the metal side, Fig. 14a, the oxide-metal interface is abrupt and appears at a depth less than 100 Å as judged by the rapid increase in the Ti signal with depth (the greatest oxide layer thickness on the metal side of any of these samples was ~ 300 Å). In Fig. 14b, the stud side, the oxide-adhesive interface is not well defined due to penetration of the adhesive into the honeycomb structure. One feature common to both depth profiles is the accumulation of F at both debonded surfaces. This was previously found near the oxide-metal interface in as-anodized and air-exposed oxides [5]. Cross-sectional TEM revealed that the oxide consisted of a 200- to 300-Å-thick barrier layer under the honeycomb structure (~ 1000-Å thick). Thus, the depth profile in Fig. 14b can be described in terms of three distinct regions: at depths less than 300 Å, the profile is dominated by the steady level of the Ti and O signals, and C is at its background level. This corresponds to the barrier layer. Between 300 and 1400 Å, the steady rise in C concentration indicates that the adhesive penetrated the oxide. At depths greater than 1400 Å, the C signal is dominant, indicative of the adhesive layer. We conclude from the micrographs and the depth profiles that the debonding occurred within the barrier layer at or very near the oxide-metal interface.

The failure at low stress levels of vacuum- and air-exposed oxides was surprising in view of the retention of the honeycomb structure after exposure. In an effort to understand this, we subsequently cycled some of the pre-exposed adherends from room temperature to 400°C several times under vacuum. The vacuum- and air-exposed adherends developed large cracks eventually whereas water-exposed adherends did not. Presumably, the cracks developed due to stress between the untransformed oxide and the base metal (at the barrier layer) during cycling. This is reasonable in that there is a 5% difference between the thermal expansion coefficients of Ti and TiO_2 [12], although a

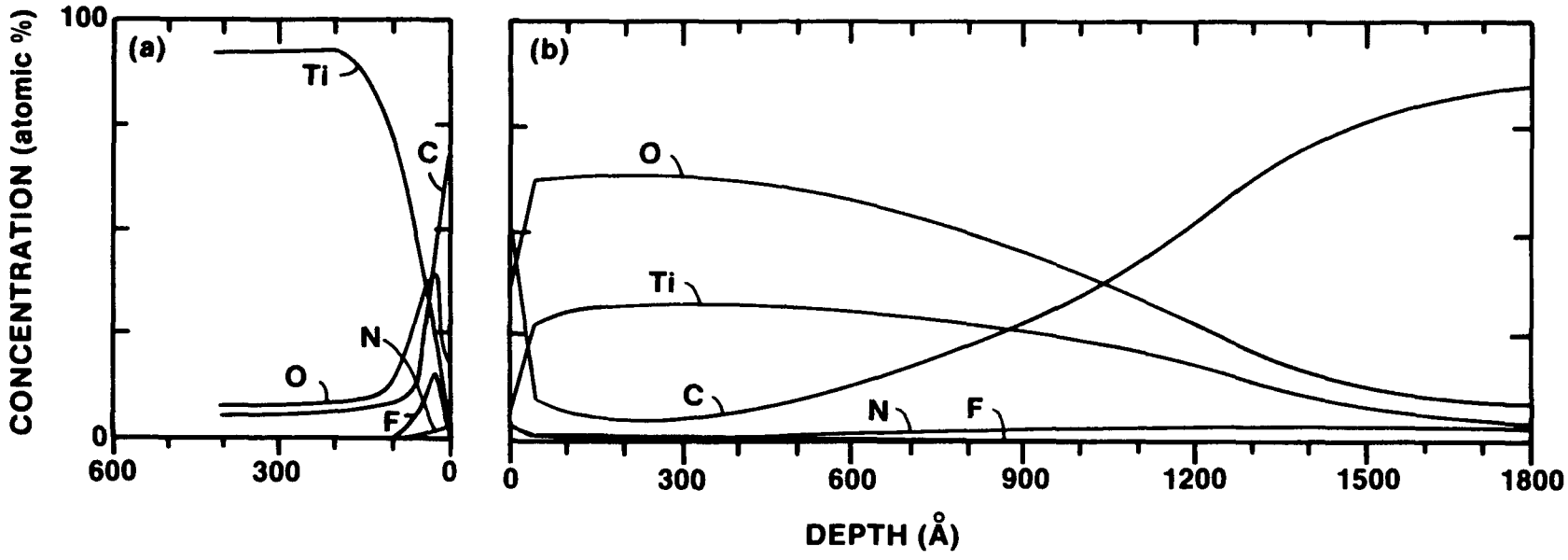

Figure 14. XPS depth profiles of the debonded surface from the a) metal and b) stud side of a Ti-6Al-4V adherend exposed to air for 1200 hr at 330°C, after tensile testing.

change in the base metal morphology during long-term exposures cannot be ruled out. Earlier cross-sectional TEM measurements of the water-exposed oxides showed that the barrier layer had disappeared with the transformation to the anatase phase [5]. Therefore, the water-exposed oxides may not have experienced the same stresses as the vacuum-exposed oxides during thermal cycling and did not develop cracks.

CAA oxides exposed to both liquid and vapor environments at temperatures below 300°C retained almost all of their bond strength, as seen in Table I. Although these debonded surfaces were not examined by XPS, the appearance of adhesive material on all of them suggests that the failure mode was predominantly cohesive in each case (although small areas of adhesive failure could be identified). It should be noted that the tensile strength values listed for water-exposed adherends in Table I represent the averages of many samples. Some of these exhibited tensile strengths comparable to those obtained for the as-anodized adherends.

Adherends exposed to humid environments at 300°C for 24 hr or more failed at low stress levels. In these cases, the two debonded surfaces appeared different, suggesting an adhesive failure mode. This was confirmed by XPS measurements. In Fig. 15a, the spectrum obtained from the metal side contains a significant concentration of Ti although the C and Si concentrations are much greater than those observed for the as-anodized surface. Two explanations for the enhanced C and Si are plausible: the increased concentrations may be due either to a very thin adhesive layer (25- to 50-Å thick) left after the tensile test or to residual solvent. The spectrum of the stud side, Fig. 15b, shows no Ti but is typical of the adhesive alone. Scanning electron micrographs show adhesive on the stud side and the nodular oxide on the metal side of the failure.

Selected area diffraction patterns obtained from water- and vapor-exposed adherends show that the oxide is crystalline TiO_2. The tensile test results indicate, at least for temperatures below 300°C, that the integrity of the oxide-metal interface is retained despite the amorphous to crystalline

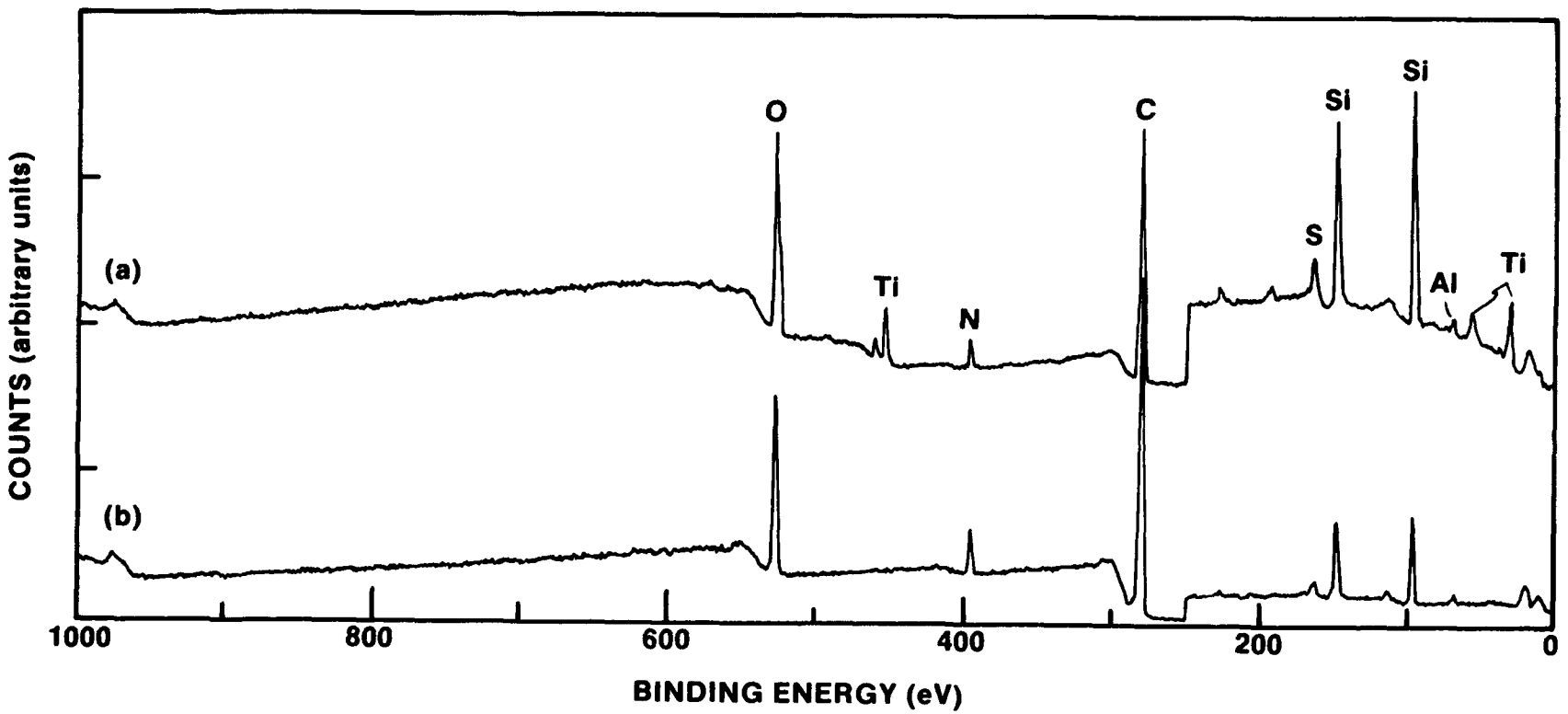

Figure 15. X-ray photoelectron spectra of a) metal and b) stud side of a Ti-6Al-4V adherend exposed to steam in a high-pressure autoclave for 120 hours at 300°C, after tensile testing.

(structural) transformation -- the transformed oxide itself can be bonded with nearly the same strength as the as-anodized oxide. This result is in contrast with those obtained for Al adherends that were exposed while bonded, in which chemical changes result in weak bonding to the base metal [2]. It is apparent from the SEM micrographs that porosity exists in water-exposed surfaces even after the transformation and, therefore, the adhesive can penetrate and interlock mechanically with the oxide.

The lack of porosity can explain the reduced bond strength in adherends exposed to humid environments for the longest times and/or at the highest temperatures. In these instances, the adhesive cannot penetrate the oxide and, therefore, no mechanical coupling can occur. The adhesive merely pulls away from the oxide under very little tensile force.

C. ALTERNATIVE SURFACE PREPARATIONS

1. Sodium hydroxide anodization (SHA)

To investigate bonding properties of surfaces produced in a non-acidic medium, Ti-6Al-4V coupons were anodized in sodium hydroxide solutions of varying concentration and temperature and at different voltages, according to reported methods [8]. The resulting adherend surfaces were characterized morphologically, chemically, and with respect to their adhesive bonding properties. Two sets of adherends, representing the extremes of the concentration range, were then exposed to high temperatures in air, pressurized water, and steam environments. Adhesive bond strengths were subsequently determined for these exposed specimens. The initial pretreatment of the adherends was identical to that used for the CAA specimens.

The surface morphologies of adherends anodized in 0.1 M and 5.0 M NaOH (10V, 30°C) are shown in Figs. 16 and 17, respectively. Both surfaces are characterized by random clusters of "crater-like" protrusions approximately 1 - 5 μm in diameter. Higher magnification reveals that the 5.0 M SHA surface

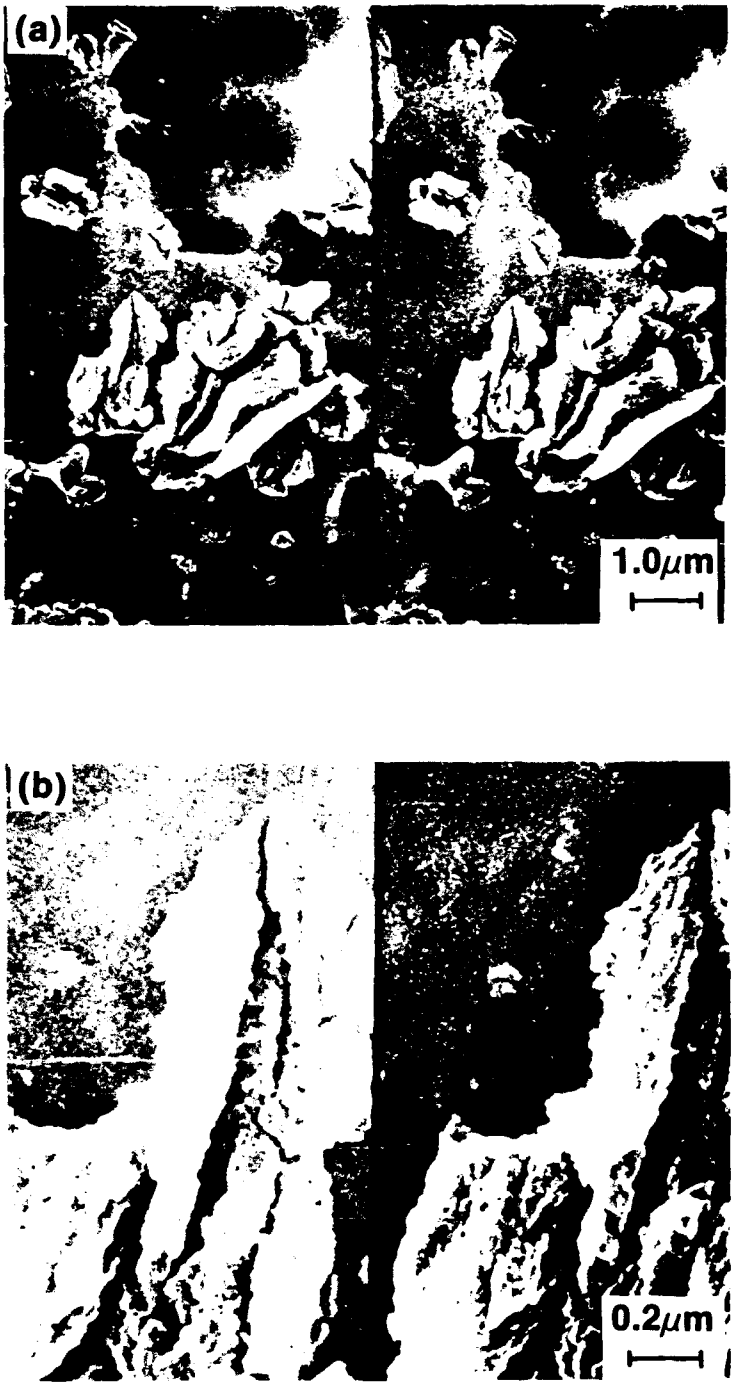

Figure 16. Morphology of Ti-6Al-4V surface after anodization in 0.1M NaOH with 10V at 30°C.

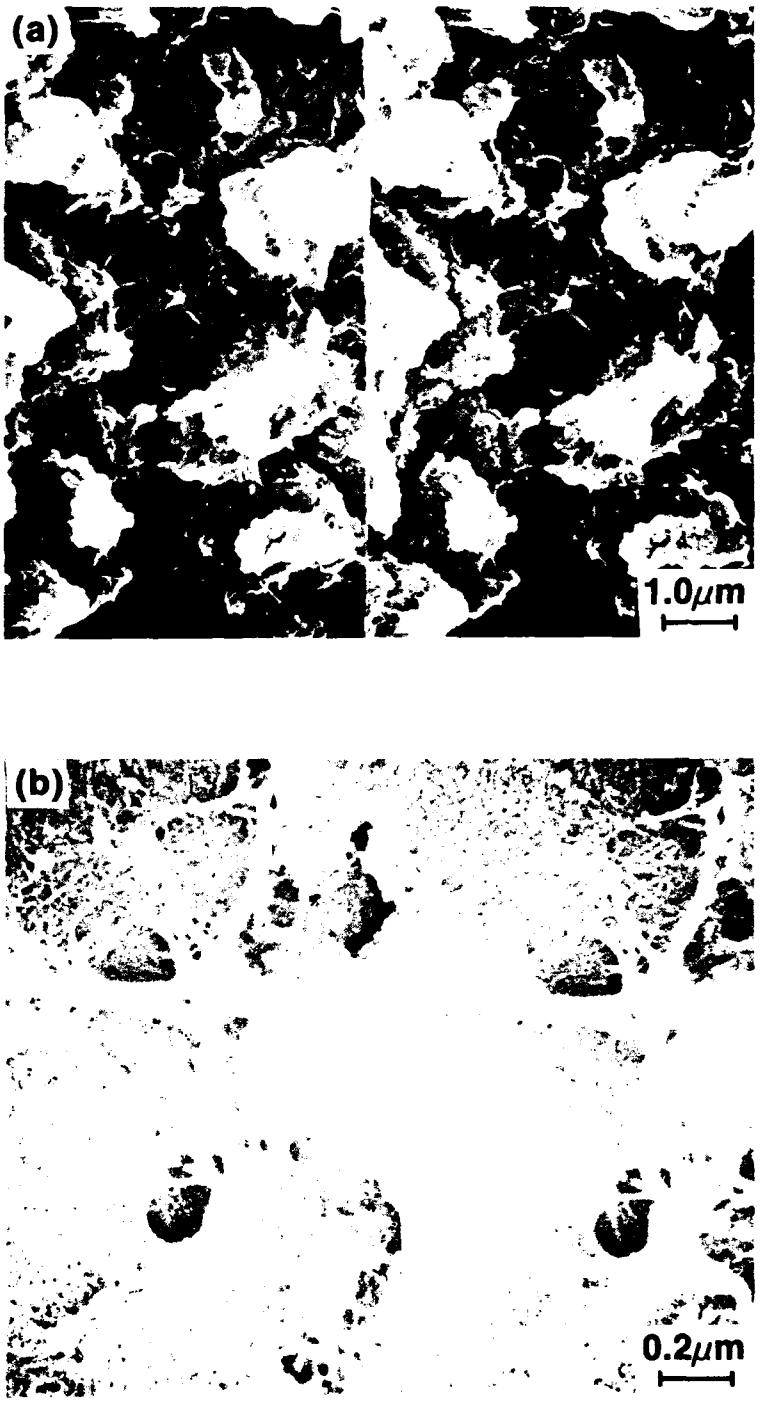

Figure 17. Morphology of Ti-6Al-4V surface after anodization in 5M NaOH with 10V at 30°C.

possesses a more complex microstructure, consisting of a semiporous "webbed" network with a regular population of cylindrical holes (approximately 0.1 μm in diameter). The 0.1 M surface appears much smoother than the corresponding 5.0 M surface, with tiny (< 0.01 μm) "bubble-like" structures defining the microroughness. Energy dispersive x-ray analysis (EDXA) of both surfaces indicated essentially equivalent quantities of the trace elements Al, V, and Cl in the specimens. Interestingly, very little Na was observed although the penetration beam depth is relatively deep (~ 1μm) and, therefore, non-surface specific. However, XPS measurements did reveal trace quantities of Na for coupons anodized in the 5.0 M NaOH solution.

The adhesive bond strengths of SHA Ti-6Al-4V adherends prepared under a variety of concentrations, voltages, and temperatures are presented in Table II. The results do not indicate significant trends, but rather show that certain sets of conditions (e.g., 0.1 M NaOH, 40°C, 10V or 5.0 M NaOH, 30°C, 15V) can produce surfaces that are comparable to the CAA surfaces with regard to tensile strength. The bonding trends and relative tensile strengths for the SHA adherends generally are comparable to results observed for corresponding exposed CAA specimens (see Table II in [6]).

The two SHA surfaces shown in Figs. 16 and 17 were chosen for subsequent environmental exposure studies because their respective morphologies and pull strength values were typical of the two (0.1 M and 5.0 M NaOH) electrolyte concentration sets studied. As with the CAA studies, the adherends were bonded after exposing the anodized surfaces in the various environments. These tensile test results are shown in Table III. In general, while the control specimens for both sets had comparable tensile strengths, the results of 5.0 M SHA exposed surfaces were significantly better than the 0.1 M SHA surfaces, in all cases. The exposure conditions included heating in air (330°C for 48 and 165 hr) and in water (300°C, 130 hr, vapor and liquid) environments.

TABLE II

Adhesion Strengths of SHA Specimens

Conditions		Average Pull Strength	
NaOH (molarity)	Temperature (°C)	(V)	(psi)
0.1 M	20	10	400
		15	600
	30	10	1100
		15	1250
	40	10	1350
		15	900
5.0 M	20	10	600
		15	1200
	30	10	1250
		15	1400
	40	10	950
		15	800

TABLE III

Adhesion Strengths of Exposed SHA Specimens

Molarity	Exposure Concitions	Average Pull Strength (psi)	Pull Strength Lost After Exposure (%)
0.1 M	Control (30°C, 10V)	1100	--
	Air (330°C): 48 hr	250	76.3
	165 hr	150	84.9
	Water (300°C, 130 hr)		
	Vapor	800	30.5
	Liquid	500	56.7
5.0 M	Control (30°C, 10V)	1200	--
	Air (330°C): 48 hr	1150	4.0
	165 hr	950	18.5
	Water (300°C, 130 hr)		
	Vapor	1100	7.8
	Liquid	550	54.3

An examination of the post-exposure SHA morphologies serves as a starting point to explain the adhesion results reported in Table III. For the air-exposed specimens (Fig. 18), the surfaces appear essentially unchanged with respect to their original structures, similar to corresponding CAA specimens. However, unlike the as-anodized specimens, which were nearly the same for both NaOH concenations, the 0.1 M adherend lost nearly 85% of it's original bond strength after the air exposure while the corresponding 5.0 M SHA coupon lost only 18.5% of it's original bond strength. This result could be directly related to porosity differences between the adherends, although other factors (e.g., oxide thickness) may also be involved. Similar bonding trends were observed for the water-exposed SHA surfaces, with both of the liquid-exposed (immersed) adherends retaining less than 50% of their pre-exposure bond strengths. Morphologically, as shown in Figs. 19 and 20, respectively, the vapor- and liquid-exposed surfaces indicate a flattened, fused-nodular appearance, similar to the corresponding CAA surfaces exposed to high-temperature aqueous conditions in the autoclave. Determination of the modes of failure for these exposed specimens is in progress and should help to elucidate the mechanism for loss of bond strengths in these adherends.

2. Additional Surface Preparations for Ti-6Al-4V

In addition to SHA, several other surface treatments, commonly used for adhesively-bonded Al alloys, have been evaluated with Ti-6Al-4V adherends. These include FPL, SMUTGO, PAA, SAA, TAA and applied Al s-butoxide. The results, presented in Table IV, show that none of the treatments was significantly better than the CAA process. Anodization in tartaric acid (TAA) and the application of Al s-butoxide to the CAA oxide surface did lead to tensile strengths which were comparable to the CAA control. While morphology studies have not yet been performed, these treatments will be investigated further as potential alternative surface preparations for the Ti-6Al-4V adherends.

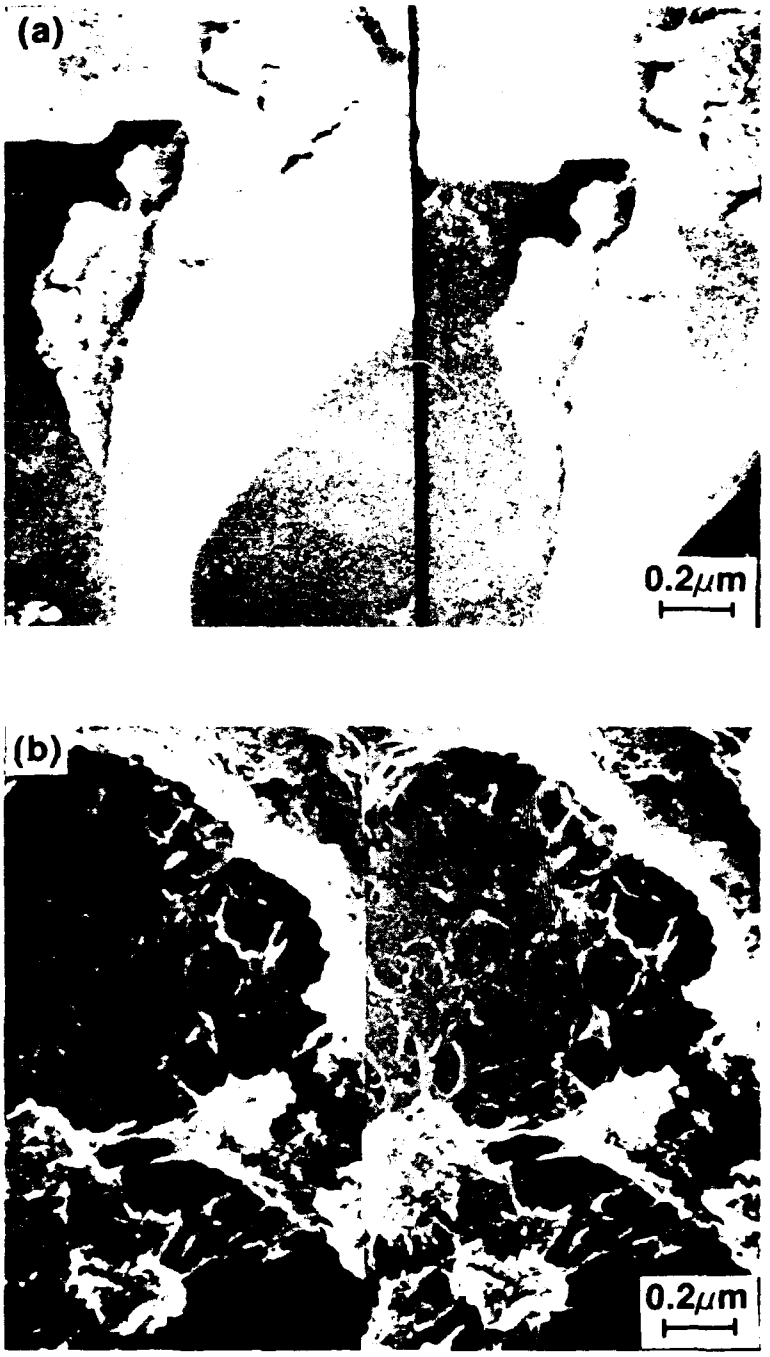

Figure 18. Morphology of Ti-6Al-4V surfaces after exposure to air at 330°C for 166 hr. Original surfaces were prepared by anodization with 10V at 30°C in (a) 0.1M and (b) 5M NaOH solutions.

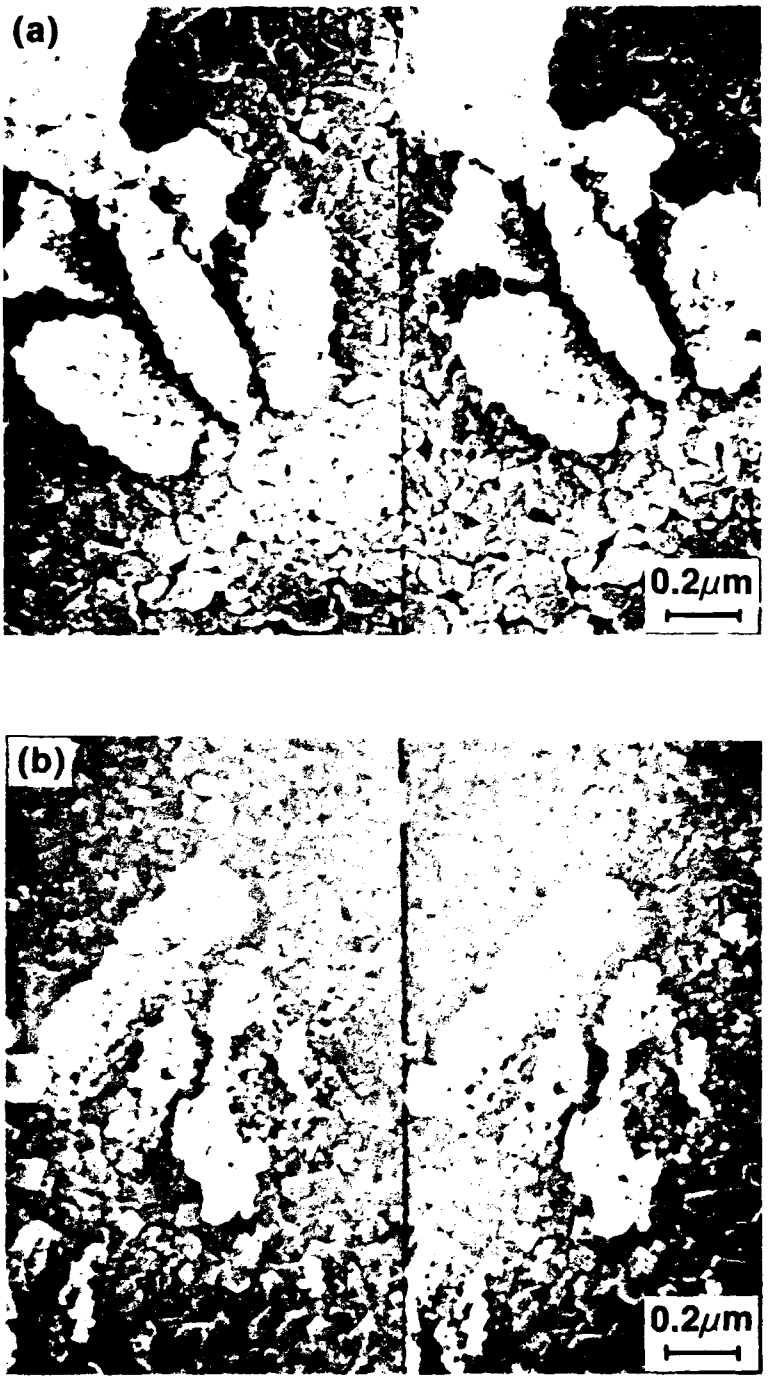

Figure 19. Morphology of Ti-6Al-4V surfaces after exposure to water vapor at 300°C for 130 hr. Original surfaces were prepared by anodization with 10V at 30°C in (a) 0.1M and (b) 5M NaOH solutions.

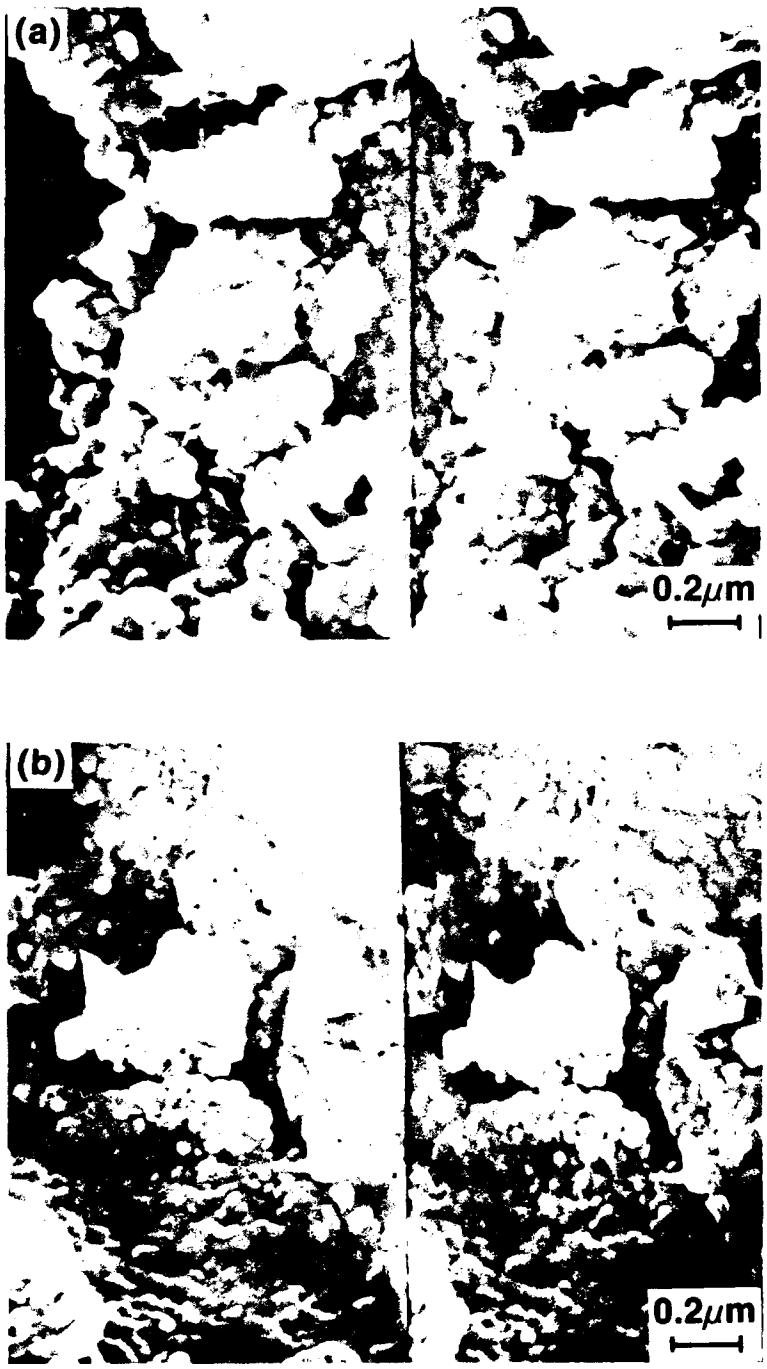

Figure 20. Morphology of Ti-6Al-4V surfaces after exposure to liquid water (immersed) at 300°C for 130 hr. Original surfaces were prepared by anodization with 10V at 30°C in (a) 0.1M and (b) 5M NaOH solutions.

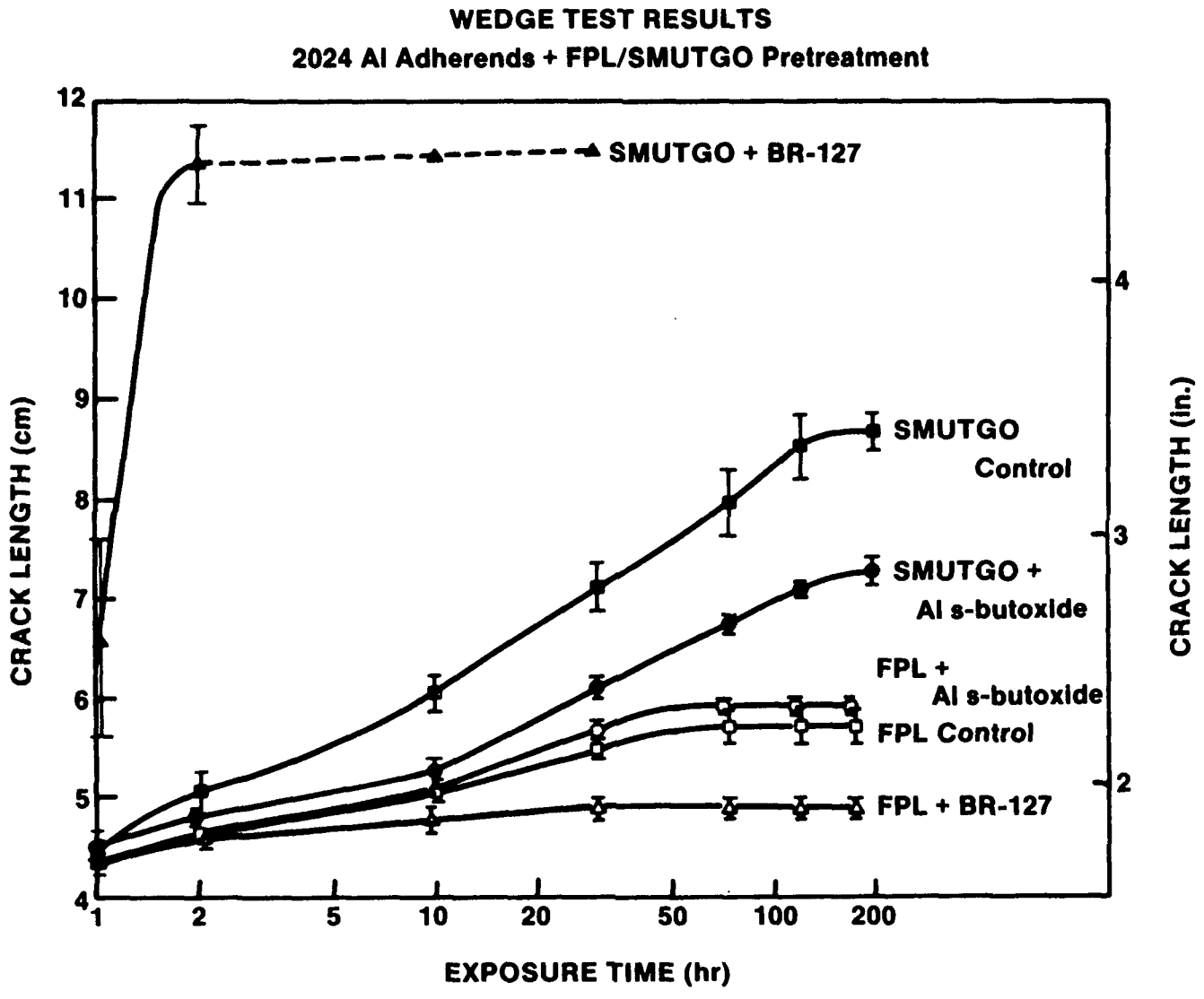

Figure 21. Wedge test results from Al 2024 T-3 adherends.

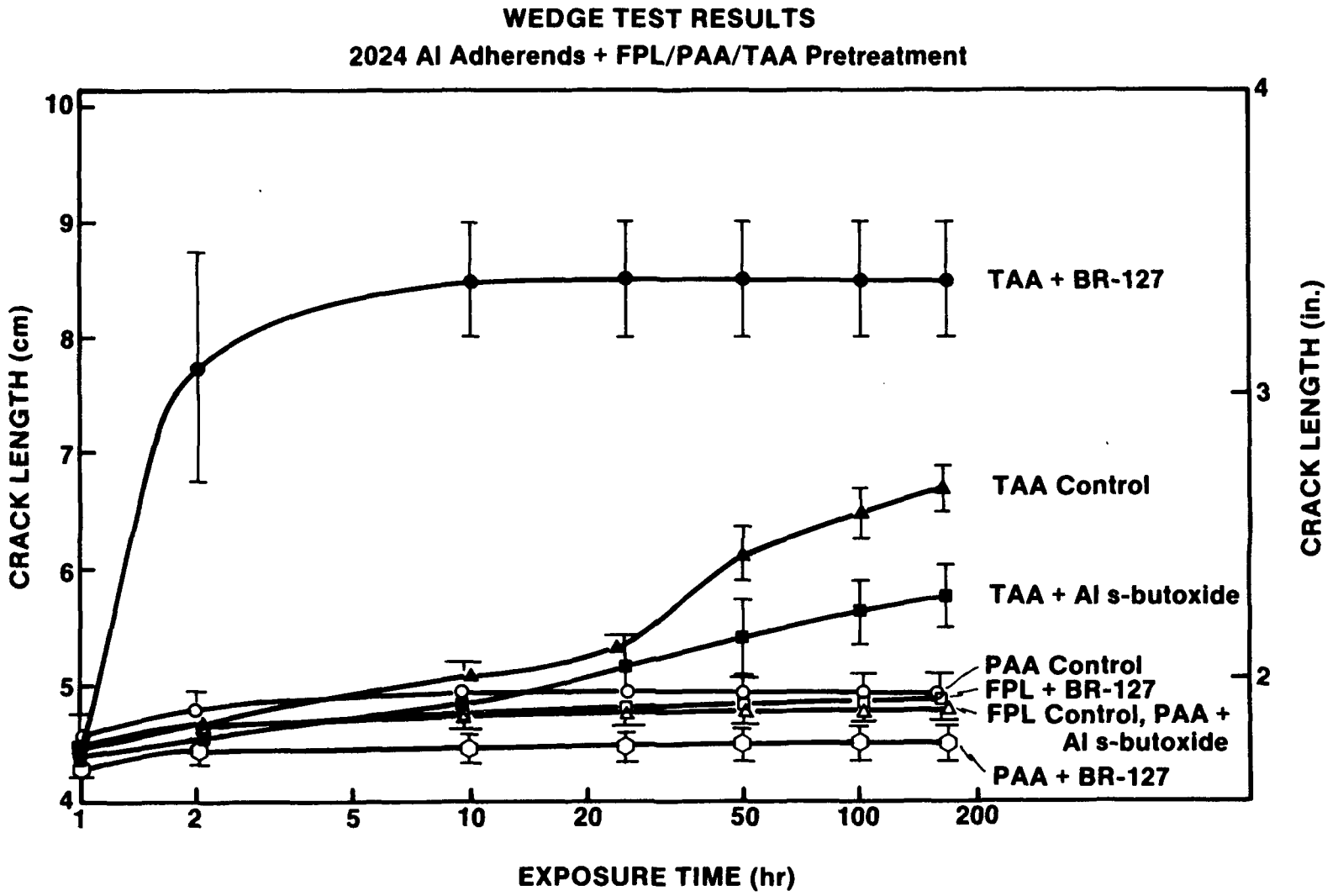

Figure 22. Wedge test results from Al 2024 T-3 adherends.

TABLE IV

Adhesion Strengths of Assorted
Ti-6Al-4V Surface Treatments

Exposure Conditions	Pull Strength (psi)
CAA Control	1400
CAA + Alkoxide	1450
FPL	750
FPL + Alkoxide	1000
SMUTGO	400
SMUTGO + Alkoxide	400
PAA	500
SAA	500
TAA	1400

3. Alkoxide Coating for the Al 2024 Alloy

The ability of an alkoxide primer to improve the bond strength between adhesive and adherend by a chemical coupling mechanism has been evaluated for two etchants and two anodization adherend pretreatments. As we reported previously [6], the application of aluminum s-butoxide [$Al(OC_4H_9)_3$] onto the surface of Al 2024-T3 pretreated with the etchants, FPL and SMUTGO, failed to improve bond durability with respect to either the FPL control or the FPL + BR-127 adhesive primer for wedge-stressed bonded systems exposed in a humid environment. However, the alkoxide did improve the bond strength and durability of the smoother SMUTGO-treated surface, suggesting that a possible coupling reaction occured between the alkoxide and the epoxy resin (see Fig. 21).

A second wedge test was performed to evaluate the alkoxide for compatability with bonded TAA, PAA, and FPL Al 2024 surfaces (Fig. 22). Once again, the microscopically rough (i.e., PAA, FPL) surfaces exhibited better bond durability than the smoother (TAA) surface. The Al s-butoxide did improve the bond durability of the TAA adherends, as it had improved the durability of the SMUTGO surface in the first test. The most durable bonded system contained the PAA + BR-127 surface (a standard production process), followed closely by the FPL control, PAA + alkoxide, FPL + BR-127, and PAA control systems. The FPL + BR-127 system performed extremely well in both wedge tests, whereas the FPL control performed better in the second test than in the first. The specimen failure modes for both wedge tests are being investigated.

IV. SUMMARY

A. ADHEREND CHARACTERIZATION

The Ti-6Al-4V alloy was anodized in 5% chromic acid solution (CAA process) to produce a consistent oxide surface for subsequent studies. The CAA oxide has been characterized as amorphous TiO_2 (TEM/SAED, XRD), with a porous, honeycomb-like morphology and two-phase (α,β) grain structure (SEM). The thickness of the oxide, determined by TEM and AES, is approximately 1200 Å, and the individual cellular diameter is approximately 600 Å (SEM, TEM).

B. ENVIRONMENTAL EXPOSURES

CAA Ti-6Al-4V adherends were exposed to high temperatures (300 - 400°C) in two "dry" environments. Specimens exposed to vacuum (400°C) for up to 165 hr retained their original morphologies, i.e., the honeycomb matrix was unchanged at the surface. For CAA surfaces exposed to ambient air (320 - 330°C) for up to 165 hr, the cell walls grew slightly thicker and some peeling of the oxide was observed near the grain boundaries.

CAA adherends were exposed to aqueous environments at temperatures ranging from 100 - 300°C. At 100°C, the growth of needle-like anatase TiO_2 crystallites proceeds until (by 72 hr.) the surface is completely covered. More severe morphological changes occur on surfaces exposed in humid environments at temperatures above 100°C in a pressurized autoclave. For example, when immersed in a liquid at 300°C, the same needle-shaped anatase crystallites grow to cover the surface, although at a much faster rate (i.e., complete coverage by 3 hr) than in boiling water. However, exposure to the steam vapor produces anatase nodules which correspond to the regular cellular pattern of the original honeycomb oxide matrix. Both surfaces progress to a flattened or "fused" nonporous morphology upon extended exposure times.

Ti-6Al-4V adherends that were previously exposed to high-temperature vacuum, air, and aqueous environments were cycled in a vacuum (< 10^{-5} torr) from room temperature to 400°C over a period of 140 hrs. The CAA control and water-exposed (liquid and vapor) surfaces appeared essentially unchanged, with their respective honeycomb, crystallite, and nodular matrix structures still intact. However, thermally cycled air- and vacuum-exposed adherends indicated a significant degree of cracking over their entire surfaces.

C. ADHESION STUDIES

Tensile testing of Ti-6Al-4V adherends that were exposed to a variety of high-temperature environments prior to testing indicates that the mode of failure depends on the nature of the environmental exposure. The as-anodized adherends all failed cohesively (within the adhesive). Although the original CAA morphology was retained after high-temperature exposures in vacuum and air, adherends subjected to these environments at temperatures greater than 320°C degraded severely and failed within the oxide layer. Oxides subjected to moderate humid environments retained almost all of their initial bond strength, although long-term high-temperature exposures resulted in adhesive (interfacial) failures. The tensile test results suggest that a pre-transformed, crystalline oxide might be used as a suitable alternative to an amorphous oxide in a bondline, since the crystalline oxide is more stable thermodynamically.

D. ALTERNATIVE SURFACE PREPARATIONS

Ti-6Al-4V adherends were anodized in solutions of sodium hydroxide (SHA) over a range of concentration, temperature, and voltage conditions. The resulting surfaces, which appeared relatively nonporous compared to corresponding CAA surfaces, were evaluated for their tensile properties before and

after high-temperature exposures in air (330°C) and water (300°C) environments. Some of the SHA adherends indicated tensile strengths that were comparable to those for CAA control specimens. However, exposed 5.0 M SHA surfaces retained a significantly higher degree of their initial bond strengths than the corresponding 0.1 M SHA surfaces, in all cases.

The ability of a primer, Al s-butoxide, to chemically enhance the bond strength between the adhesive and an Al 2024-T3 adherend surface was evaluated by environmental wedge tests. In general, the primer tended to improve adhesion for smoother (e.g., SMUTGO, TAA) morphologies, but actually weakened the bond strength for microscopically rough (FPL, PAA) oxide surfaces.

V. ACKNOWLEDGEMENTS

We acknowledge useful discussions with D. McNamara, G. Davis and J. Venables. G. Cole acquired much of the XPS data. P. Martin assisted with the tensile tests and A. Desai assisted with the wedge tests. The financial support of DARPA/ONR under contract number N00014-85-C-0804 is gratefully acknowledged.

VI. REFERENCES

1. B.M. Ditchek, K.R. Breen, T.S. Sun, and J.D. Venables, al. Proc. 25th Natl. SAMPE Symp. Exhib., p.13, San Diego, CA, 1980 (SAMPE, Azusa, CA, 1980).

2. J.D. Venables, D.K. McNamara, J.M. Chen, T.S. Sun, B.M. Ditchek, T.I. Morgenthaler, and R. Hopping, Proc. 12th Natl. SAMPE Tech. Conf., p. 882, Seattle, WA, 1980 (SAMPE, Azusa, CA, 1980).

3. D.A. Hardwick, J.S. Ahearn, A. Desai and J.D. Venables, J. Mater. Sci. 21, 179 (1986).

4. M. Natan and J.D. Venables, J. Adhes. 15, 125 (1983).

5. H.M. Clearfield, D.K. Shaffer and J.S. Ahearn, accepted for publication in 18th Natl. SAMPE Tech. Conf., Seattle, WA, Oct. 7-9 (1986).

6. D.K. Shaffer, H.M. Clearfield, and J.S. Ahearn, MML TR86-42c, Quarterly Report No. 3, Martin Marietta Laboratories, under Contract No. N00014-85-C-0804,

7. A. Matthews, Am. Mineral. 61, 419 (1976).

8. A.C. Kennedy, R. Kohler, and P. Poole, Int. J. Adhes. and Adhes. 3, 133 (1983).

9. R.A. Pike, Int. J. Adhes. and Adhes. 6 (No. 1), 21 (1986).

10. Y. Moji and J.A. Marceau, U.S. Patent No. 3959091, assigned to the Boeing Company (1976).

11. P.A. Redhead, J.P. Hobson, and E.V. Kornelsen, The Physical Basis of Ultrahigh Vacuum (Chapman and Hall, London, 1968).

12. A. Goldsmith, H.J. Hirschhorn, and T.E. Waterman, Thermophysical Properties of Solid Materials, Vol. II, WADC Tech. Rep. 58-476 (Wright Air Development Division, Dayton, OH, 1960).

13. L.S. Hsu, R. Rujkorakarn, J.R. Sites, and C.Y. She, J. Appl. Phys. 59, 3475 (1986).

MARTIN MARIETTA

Martin Marietta Laboratories
1450 South Rolling Road
Baltimore, Maryland 21227
(301) 247-0700